

**Best
Available
Copy**

AD-773 389

DESIGN AND DEVELOPMENT OF A SEG-
MENTED MAGNET HOMOPOLAR TORQUE
CONVERTER

C. J. Mole, et al

Westinghouse Electric Corporation

Prepared for:

Advanced Research Projects Agency

January 1974

DISTRIBUTED BY:

NTIS

National Technical Information Service
U. S. DEPARTMENT OF COMMERCE
5285 Port Royal Road, Springfield Va. 22151

E.M. 4559

DESIGN AND DEVELOPMENT OF A
SEGMENTED MAGNET HOMOPOLAR TORQUE CONVERTER

Semi-Annual Technical Report for
Period Ending November 30, 1973

Submitted to ARPA in January 1974

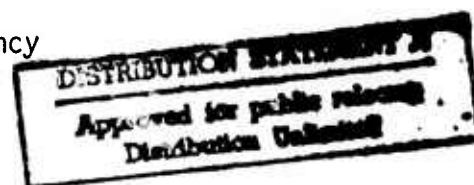
Principal Investigator:

C. J. Mole

C. J. Mole, Mgr.
Superconducting Electrical Machinery Systems
Phone (412) 256-3612

Sponsored by:

Advanced Research Projects Agency
ARPA Order No. 2174



This research was supported by the Advanced Research Projects Agency of the Department of Defense under Contract No. DAHC 15-72-C-0229. Contract expiration date 1 March 1974. Amount of contract - \$1,129,969. Effective date of Contract 10 May 1972.

Westinghouse Electric Corporation
Electro-Mechanical Division
P.O. Box 217
Cheswick, PA 15024

ib

Unclassified

Security Classification

DOCUMENT CONTROL DATA - R & D

(Security classification of title, body of abstract and indexing annotation must be entered when the overall report is classified)

1. ORIGINATING ACTIVITY (Corporate author) Westinghouse Electric Corporation Electro-Mechanical Division Cheswick Avenue, Cheswick, PA 15024		2a. REPORT SECURITY CLASSIFICATION Unclassified	
		2b. GROUP	
3. REPORT TITLE DESIGN AND DEVELOPMENT OF A SEGMENTED MAGNET HOMOPOLAR TORQUE CONVERTER			
4. DESCRIPTIVE NOTES (Type of report and inclusive dates) Semi-Annual Technical Report for period ending November 30, 1973			
5. AUTHOR(S) (First name, middle initial, last name) Mole, C.J. and Arcella, F.G.; Berkey, E.; Boes, D.J.; Feranchak, R.A.; Haller, H.E. III; Johnson, J.L.; Karpathy, S.A.; Keeton, A.R.; Litz, D.C.; Mullan, E.; Reichner, P.; Tsu, T.C.; Ulke, A.; Witkowski, R.E.			
6. REPORT DATE January 1974		7a. TOTAL NO. OF PAGES 98 85	7b. NO. OF REFS 14
8a. CONTRACT OR GRANT NO. DAHC 15-72-C-0229		9a. ORIGINATOR'S REPORT NUMBER(S) E.M. 4559	
b. PROJECT NO.		9b. OTHER REPORT NO(S) (Any other numbers that may be assigned this report)	
c.			
d.			
10. DISTRIBUTION STATEMENT Qualified requesters may obtain copies of this report from Defense Documentation Center, Cameron Station, Alexandria, Virginia 22314			
11. SUPPLEMENTARY NOTES		12. SPONSORING MILITARY ACTIVITY Advanced Research Projects Agency Department of Defense 1400 Wilson Blvd., Arlington, VA 22209	
13. ABSTRACT This program is for the research and development of a new mechanical power transmission concept: the segmented magnet homopolar torque converter. The purpose of this device is to convert unidirectional torque of constant speed (such as from a steam turbine prime mover) into variable speed output torque in either the forward or reverse directions. The concept offers an efficient, lightweight low volume design with potential application over a wide range of speeds and power ratings in the range from hundreds to tens of thousands of horsepower. This machine concept can be applied to commercial and military advanced concept vehicles for both terrain and marine environments. The program places particular emphasis on the materials technology of liquid metal current collection systems for the reason this is essential for the success of the homopolar machine concept. This report period encompasses the initiation of Phase II experimental work. In Phase I the technical problems were reviewed, the machine concepts were studied, and a detailed technical plan was evolved for the entire program. In Phase II, theoretical, engineering, and experimental tasks will be performed to develop a reliable current collection system which will be demonstrated in an actual segmented magnet homopolar generator.			

Reproduced by
NATIONAL TECHNICAL
INFORMATION SERVICE
U S Department of Commerce
Springfield VA 22151

DD FORM 1 NOV 65 1473

Unclassified

Security Classification

Unclassified

Security Classification

14 KEY WORDS	LINK A		LINK B		LINK C	
	ROLE	WT	ROLE	WT	ROLE	WT
alkali metals dc motor electric machine homopolar liquid metals motor ship propulsion torque converter						

ia

Unclassified

Security Classification

The views and conclusions contained in this document are those of the authors and should not be interpreted as necessarily representing the official policies, either expressed or implied, of the Advanced Research Projects Agency or the U. S. Government.

TABLE OF CONTENTS

	<u>Page</u>
Section 1 INTRODUCTION AND SUMMARY-----	1-1
1.0 General-----	1-1
1.1 Background-----	1-1
1.2 Objectives-----	1-1
1.2.1 Summary of Objectives-----	1-1
1.2.2 Summary of Technical Tasks-----	1-2
1.3 Summary of Current Progress-----	1-4
1.3.1 Machine Design and Testing-----	1-4
1.3.2 Application Studies-----	1-4
1.3.3 Liquid Metal Current Collection Systems--	1-4
1.3.4 Liquid Metal Support Systems-----	1-5
1.3.5 Seal Studies-----	1-6
2 MACHINERY-----	2-1
2.1 Segmented Magnet Homopolar Machine (SEGMAG)-----	2-1
2.1.1 Objectives-----	2-1
2.1.2 Prior and Related Work-----	2-1
2.1.3 Current Progress-----	2-1
2.2 GEC Generator-----	2-4
2.2.1 Objectives-----	2-4
2.2.2 Prior and Related Work-----	2-4
2.2.3 Current Progress-----	2-4
3 APPLICATION STUDIES-----	3-1
3.0 Objectives-----	3-1
3.1 Prior and Related Work-----	3-1
3.2 Current Progress-----	3-1
4 CURRENT COLLECTION SYSTEMS-----	4-1
4.0 Objectives-----	4-1
4.1 Prior and Related Work-----	4-1
4.1.1 Power Loss Considerations-----	4-1
4.1.2 Confinement Considerations-----	4-2
4.2 Current Progress-----	4-2
4.2.1 Experimental Program Test Parameters-----	4-3
4.2.2 Preliminary Experiments with Small Test Rigs-----	4-8
4.2.3 Large Test Rig-----	4-12
4.2.4 Experiments with Large Test Rig-----	4-12
4.2.5 Fluid Flow Considerations-----	4-16
4.3 References-----	4-23
5 LIQUID METAL SUPPORT SYSTEMS-----	5-1
5.0 Objectives-----	5-1
5.1 Prior and Related Work-----	5-1
5.2 Current Progress-----	5-1

Table of Contents (cont'd.)

	<u>Page</u>
5.2.1 Materials Selection and Compatibility Studies-----	5-1
5.2.2 Liquid Metal Loop and Cover Gas Systems--	5-12
5.3 References-----	5-22
6 SEAL STUDY-----	6-1
6.0 Objectives-----	6-1
6.1 Prior and Related Work-----	6-1
6.2 Current Progress-----	6-2
6.2.1 Face Seal Screening Tests-----	6-5
6.2.2 Functional Testing: Tandem Circumferential Seal-----	6-10
6.3 References-----	6-12

REFERENCES

References are listed at the end of each section.

LIST OF FIGURES

<u>Figure</u>		<u>Page</u>
2-1	SEGMAG Components	2-3
2-2	GEC Homopolar Open Circuit Tests	2-6
2-3	GEC Homopolar Motor Tests	2-6
2-4	GEC Homopolar Short Circuit Tests	2-7
2-5	GEC Generator Load Test	2-7
4-1	Liquid Metal (NaK-78) Current Collector Power Losses from Magnetic Field Effects	4-7
4-2	Liquid Metal Current Collector Test Stand	4-13
4-3	Viscous Torque-NaK Flow Characteristics for Rotating Disk Collector ϵ	4-15
4-4	Comparison of Experimentally Determined and Calculated Viscous Power Loss-Speed Characteristics for Rotating Disk Collector ϵ	4-15
4-5	Critical Performance-Temperature Curve for Rotating Disk Collector ϵ	4-15
4-6	Test Collector ϵ After 76-hour Run in Glove Box	4-17
4-7	Distribution of the States of Flow as Functions of the Reynolds Number and the Taylor Number	4-19
5-1	Glove Box Facilities Utilized for the Preparation and Handling of Materials Being Evaluated for NaK Compatibility	5-3
5-2	Constant Temperature Oil Bath Facilities for the Isothermal Ageing of Materials in an NaK Environment	5-4
5-3	Simplified Flow Chart of Materials Compatibility Test Plan	5-5
5-4	Rotor Banding Material 431-S-2 (Epoxy Novalac Resin/ Glass Fibers) Before and After NaK Exposure at 140°C for 507.5 Hours	5-6
5-5	Resistivity Measurements Obtained on Heat Aged and NaK Exposed Electrical Insulation Systems	5-8

List of Figures (cont'd.)

5-6	Silastic Elastomers (116 RTV and RTV 732) Before and After NaK Exposure at 140°C for 100 Hours	5-10
5-7	The Change in Ultimate Stress and Elastic Modulus of Candidate Laminate Materials as a Result of NaK Exposure at 140°C	5-11
5-8	Braze Alloy B Cu P-5 (15 Ag-80 Cu-5 P) Before and After NaK Exposure at 140°C for 112 Hours	5-13
5-9	Braze Alloy B Au-4 (81.5 Au-18.5 Ni) Before and After NaK Exposure at 140°C for 112 Hours	5-14
5-10	Small Loop Concept to Service Each Current Collector Independently	5-15
5-11	Calibration of NaK Flowmeter for 35.6 cm Current Collector Test Stand	5-15
5-12	Assembled NaK Loop for Current Collector Service for Prototype SEGMAG Machine	5-16
5-13	Illustrating Placement of Six Current Collection NaK Loops Beneath SEGMAG machine	5-16
5-14	Prototype SEGMAG Generator Cover Gas System	5-20
5-15	Internal Components of Central Gas Purifier Station for the SEGMAG Homopolar Machine	5-21
6-1	Schematic of Typical Tandem Circumferential Seal	6-3
6-2	Shaft/Containment Vessel Seal Test Stand	6-3
6-3	Details of Seal Test Device	6-4
6-4	Tandem Circumferential Seal Test Rig	6-4
6-5	Face Seal Screening Test Apparatus	6-6
6-6	Operating Temperature and Friction Coefficient vs Time for WSe ₂ /GaIn Seal Material-15 psi-2360 fpm-N ₂	6-8
6-7	Operating Temperature vs Time for SP-3 Seal Material-2.6 psi-2360 fpm-He	6-8

List of Figures (cont'd.)

6-8	Operating Temperature and Friction Coefficient vs Time for SP-211 Seal Material - 2.6 psi- 2360 fpm-N ₂	6-9
6-9	Operating Temperature and Friction Coefficient vs Time for Meldin PI-30 Seal Material - 15 psi- 2360 fpm-N ₂	6-9
6-10	Photograph of Tandem Circumferential Seal-Bore: 3.97" Diameter	6-11
6-11	Leak Rate vs Running Time for Tandem Circumfer- ential Seal Operating in Dry N ₂ 2100 rpm-5psig Feed Gas	6-11

LIST OF TABLES

<u>Table</u>		<u>Page</u>
4-1	Calculated Power Losses in Current Collector Related to Axial Magnetic Field and Radial Gap	4-5
4-2	Calculated Power Loss in Current Collector Related to Radial Magnetic Field and Radial Gap	4-7
4-3	Summary of Small Current Collector Designs	4-10
4-4	Summary of Prototypic Size Collector Designs	4-13
4-5	Data for Critical Reynolds Number Calculations	4-19
4-6	Calculated Reynolds Number for Critical Flow Conditions	4-19
4-7	Dimensionless Fluid Flow Characterizing Numbers	4-22
5-1	Rotor Banding Material 431-S-2 (Epoxy Novalac Resin/Glass Fibers) Tensile Test Data	5-7
5-2	Braze Alloys Evaluated for NaK Compatibility at 140°C	5-9
5-3	NaK Loop Capabilities	5-18
5-4	NaK Loop Endurance Test	5-18
5-5	Cover Gas System Capabilities	5-21
6-1	Candidate Seal Materials for Use in SEGMAG Primary Rotor Shaft Seals	6-5
6-2	Face Seal Test Results on Candidate Seal Materials	6-7
6-3	Friction-Wear Characteristics of Candidate Seal Materials Pre- and Post NaK Exposure	6-8

SECTION 1

INTRODUCTION AND SUMMARY

1.0 GENERAL

This is the third semi-annual technical report and covers the work performed from June 1, 1973 through November 30, 1973. During this period, the Phase II workscope was pursued in accordance with the agreed plan.

1.1 BACKGROUND

This program is for the research and development of a Westinghouse-proposed mechanical power transmission concept: the segmented magnet homopolar torque converter (SMHTC). The purpose of this device is to convert unidirectional torque of constant speed (such as from a steam turbine prime mover) into variable speed output torque in either the forward or reverse directions. The concept offers an efficient, light-weight low volume design with potential application over a wide range of speeds and power ratings in the range from hundreds to tens of thousands of horsepower. Initial analysis indicates that this machine concept can be applied to commercial and military advanced concept vehicles for both terrain and marine environments over a wide range of applications with considerable benefit to the U.S. Government, provided the complex current collection, liquid metal technology, and materials problems can be completely solved.

The present contract is part of a proposed three phase program to develop the segmented magnet homopolar torque converter (SMHTC). This program will, a) solve the operational problems relating to current collection systems for segmented magnet machines; b) demonstrate the solution of these problems in a small segmented magnet homopolar machine (SEGMAG); c) utilize the developed technology to design, construct and test a segmented magnet homopolar torque converter (SMHTC).

The program will place particular emphasis on the materials technology of liquid metal current collection systems for the reason that this is essential to the success of the homopolar machine concept for high power density applications.

1.2 OBJECTIVES

1.2.1 Summary of Objectives

In Phase I, completed on January 9, 1973, all of the technical problems were reviewed, the machinery concepts studied, and a detailed technical plan was evolved for Phase II.

Phase II has the primary purpose of providing the necessary theoretical and engineering design work, as well as the supporting experimental tasks, to develop a reliable and efficient current collection system for the successful operation of a segmented magnet (SEGMAG) homopolar generator. Key task areas include: (a) the design, construction, and operation of a SEGMAG generator having sodium-potassium (NaK) current collectors and all necessary support systems for liquid metal handling and purification, cover gas purity maintenance, and shaft seals; and (b) the procurement and testing of a GEC Ltd. homopolar generator with its Gallium-Indium (GaIn) current collector system.

The objectives of Phase III will be to extend the technology developed in Phase II for constant speed machines (such as generators) to the case of a torque converter which operates at low speed, zero speed, or reversing conditions, and then to construct and test a demonstration machine.

1.2.2 Summary of Technical Tasks

The technical subtasks for Phase I were described in detail in the first semi-annual technical report (E.M. 4471), and are as follows:

- 1) Segmented magnet homopolar torque converter (SMHTC) system studies.
- 2) Application study.
- 3) Liquid metal current collection systems.
- 4) Materials study.
- 5) Segmented magnet homopolar machine design.
- 6) Seal study.
- 7) Plan for phase II

There are five major task areas under Phase II:

(1) Machine Design and Testing

A segmented magnet homopolar machine (rated 3000 HP, 3600 rpm) will be designed, constructed, and tested. This development will prove the concept and allow testing of improvements for areas such as the current collectors, seals, and materials. Extensive testing will be conducted.

A homopolar generator will be obtained from the General Electric Co. (GEC) of England. The prime purpose is to obtain operational experience with GaIn as a current collector liquid. This machine's mechanical and electrical design and performance will be studied as a basis for evaluating presently used models for predicting machine performance.

(2) Application Studies

Several of the applications resulting from the Phase II application studies will be reviewed in conjunction with ARPA, and the most useful applications for segmented magnet homopolar machines or torque converters will be selected.

(3) Current Collection Development

The purpose of this task is to evolve an effective liquid metal current collection system and to evaluate its performance. The principal areas of study concern handling, containment, removal of contaminants, and measure of power losses.

(4) Liquid Metal Support Systems

The purpose of this task area is to develop, design, fabricate, and instrument a liquid metal recirculation loop and a cover gas recirculation system to provide maximum protection to the liquid metal in the current collector region. Both the liquid metal and the cover gas will be recirculated for contaminant removal and purity maintenance. Consideration will be given to use of these systems for removal of waste heat from the machine.

This task includes a compatibility study of all machine materials (insulation, lubricants and structural materials) with the liquid metal current collection fluid.

A fundamental studies program is part of this task area and is concerned with those aspects of liquid metal technology that are necessary to optimize the current collection electrodes to provide long term reliability for stable current conduction. Topics include surface wetting by liquid metals, aerosol formation, corrosion or alloying reactions, effect of high current transfer, and chemistry control in liquid metals using soluble getters.

(5) Seal Study

In this task seal systems will be developed to: (a) confine the liquid metal to the collector zone; and (b) prevent air contamination of the liquid metal and loss of its protective cover gas atmosphere. Test rigs will be constructed to simulate actual machine operating conditions.

1.3 SUMMARY OF CURRENT PROGRESS

1.3.1 Machine Design and Testing

1.3.1.1 Segmented Magnet Homopolar Generator (SEGMAG)

The electrical and mechanical designs of the SEGMAG were completed. Most of the major material items necessary for the construction of the machine were received, and fabrication was initiated. Significant portions of the manufacturing have now been completed.

The test stand for the SEGMAG was designed and fabricated. The necessary drive motor, gear box, and field exciter motor-generator set was ordered and received. Installation of the test stand, as well as all auxiliary equipment for electrical power, water cooling, cover gas supply, liquid metal supply, instrumentation and control, is nearing completion.

1.3.1.2 GEC Machine

The GEC generator was completed in late October and performance tested at the GEC Labs in the presence of two Westinghouse engineers prior to shipment. The machine operated satisfactorily during all tests and was accepted for delivery. The machine is scheduled to arrive at the Westinghouse R&D Center in mid-December. A test stand is being designed to support the machine for testing during 1974.

1.3.2 Application Studies

The basic advantages of segmented magnet homopolar machines were reviewed, and based on these advantages, a number of promising application areas were identified for further investigation.

1.3.3 Liquid Metal Current Collection Systems

Experimental test apparatus suitable for evaluating liquid metal current collectors under controlled operating conditions was fabricated and experiments to achieve a viable collector were initiated. Based on electrical, hydrodynamic, and magnetohydrodynamic (MHD) considerations, the two most important collector test conditions to be simulated in view of the SEGMAG application are rotor disk speed and radial magnetic field intensity. These independent variables are controllable with the experimental test facilities to levels of 78 m/s and 0.1 Tesla, respectively. The latter test capability is three times greater in magnitude than that anticipated to be present in the SEGMAG demonstration generator. This test provision was incorporated so that a better quantitative evaluation of the power loss associated with the radial magnetic field effect can be made. Evaluations are being made on prototypic size

current collectors with 35.6 cm diameter rotors, eliminating the need to apply scaling law factors to collector designs for the SEGMAG generator application.

Experimental tests to date reveal that the flow rate of liquid metal (NaK-78) into and out of the collector is controllable. No evidence of collector flooding was shown with NaK flow rates to $13 \text{ cm}^3/\text{s}$ and rotational speeds to 67 rps. Confinement of liquid metal to the collection zone during rotational speeds in the range of 10 to 67 rps has been demonstrated a number of times with two recent collector designs. During an extended run of 76 hours, at a constant rotor disk speed of 60 rps, the loss of liquid metal from the collector was estimated to be one part in three million. Pre and post-test chemical analyses of the liquid metal failed to reveal any change from its original eutectic composition as a result of the prolonged viscous working. Although desirably lower than predicted, good agreement was obtained between the measured and calculated values of ordinary hydrodynamic power loss.

During the course of experimental work, current collector performance was found to be critically dependent on temperature. Good performance was observed, in terms of gap filling and confinement of liquid metal to the collector, if operation occurred at temperatures above a critical level for each speed. Operation below the critical temperature caused an adverse effect on collector performance.

Continuing effort is underway to substantiate that an experimental solution to the liquid metal current collection problem for generator applications has been achieved. This effort will include an evaluation of (1) radial field effects on power loss, (2) joulean and viscous work effects on chemical integrity of the liquid metal, and (3) a simulation of load current effects on liquid confinement to the collection zone.

1.3.4 Liquid Metal Support Systems

A prototype liquid metal recirculation and purification loop has been designed, fabricated, and endurance tested to over 2000 hours operation under adverse operating conditions. Six SEGMAG loops have been fabricated. A protective cover gas recirculation and purification system has been designed, fabricated, and is undergoing qualification testing. The cover gas-liquid metal interaction window is being analyzed to define optimum operating conditions. Machine applicable decontamination and safety techniques have been devised and verified through practice on the 35.6 cm current collector test stand. Automated, subsystem instrumentation and controls were designed, constructed, and operationally proven on the 35.6 cm current collector test stand.

A literature survey of the current state-of-the-art, defining materials which are compatible with NaK, has been completed. A test plan for the evaluation of candidate SEGMAG materials with NaK was defined, written, and put into effect. Candidate materials have been selected, and their NaK compatibility evaluation is near completion. Electrical insulation and organic material outgassing species have been identified. The SEGMAG decontamination scheme has been defined and tested on the proposed construction materials. GaIn compatibility studies are being initiated.

1.3.5 Seal Studies

Face seal screening tests on candidate seal materials for the primary rotor shaft seals of SEGMAG indicated that two polyimide matrix composites exhibit satisfactory friction-wear characteristics in the inert, no-moisture environment required for SEGMAG. The composites contain solid lubricants, such as molybdenum disulphide, Teflon, and graphite, as fillers. Both materials have also been found to be compatible with the liquid metal NaK at a temperature of 108°C. Seal segments suitable for use in tandem circumferential seals are currently being fabricated from these materials.

A total of four tandem circumferential seals was purchased for functional testing purposes as well as for use on the SEGMAG prototype machine. Functional testing on these units has indicated that seal leak rates can be held to 0.02 cfm or less. Functional tests have also graphically illustrated that the use of carbon-graphite seal materials in these units is unsatisfactory when they are applied in dry, inert gas environments.

SECTION 2 MACHINERY

2.1 SEGMENTED MAGNET HOMOPOLAR MACHINE (SEGMAG)

2.1.1 Objectives

The objective of this program is to demonstrate the SEGMAG concept and to provide a test vehicle for evaluation of the current collection systems, containment seals, and liquid metal handling systems developed in previous subassembly testing. The demonstration unit (rated 3000 HP, 3600 RPM) will subject the current collectors to current densities, leakage flux and other conditions associated with operation in a machine environment. In addition, the unit will provide for long-term testing of current collectors, their attendant support systems and the machine itself to develop operational data for liquid metal machines.

2.1.2 Prior and Related Work

The SEGMAG concept was developed to provide a high performance DC machine without requiring superconducting magnet excitation. This low reluctance machine, using room temperature excitation, has capability for high output per unit weight and volume. The modular construction allows for higher outputs by using many modules connected in series. The characteristics of this machine have been investigated thoroughly in another U. S. Government Contract (N000 14-72-C-0393).

2.1.3 Current Progress

The electrical and mechanical design of the SEGMAG demonstration unit is complete. Detail drawings have been completed for all of the major subassemblies except the excitation coils. The layout drawing for the coils is complete and the detailed drawings are being developed.

The discovery of a critical temperature for acceptable operation of the current collectors has necessitated a re-evaluation of the thermal design of the machine. The critical temperature for proper operation at 3600 rpm is 78°C. Using this as a lower bound for collector temperature, a machine current of 80,000 amps is achievable. If the current is increased above 80,000 amps and the maximum hot spot temperature is maintained at 130°C, the collector temperature is lowered below the critical temperature of 78°C. Additional work is planned to determine if the generator current can be raised above 80,000 amps.

The demonstration SEGMAG machine is presently being fabricated with an anticipated completion date of January 31, 1974. The status of various subassemblies is listed below:

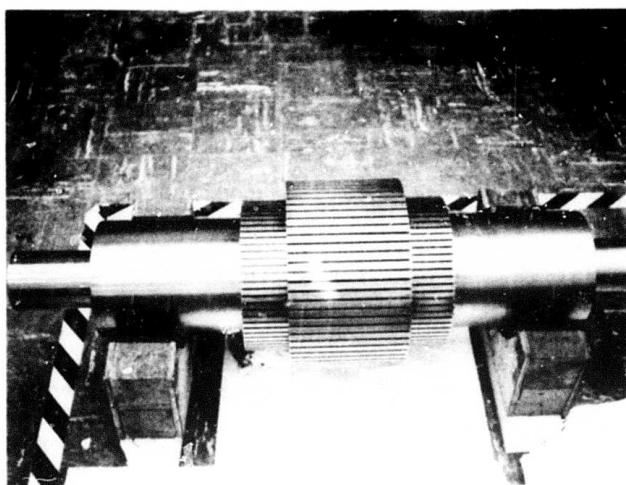
- Rotor - All material for rotor construction has been received. The rotor and two end modules have been semi-finish machined

and slotted for rotor bars. See Figure 2-1. The rotor bars have been finished machined. The rotor collector rings are presently being machined and slotted. Braze mockups of the module insulation and collector ring to rotor bar have been successfully tested.

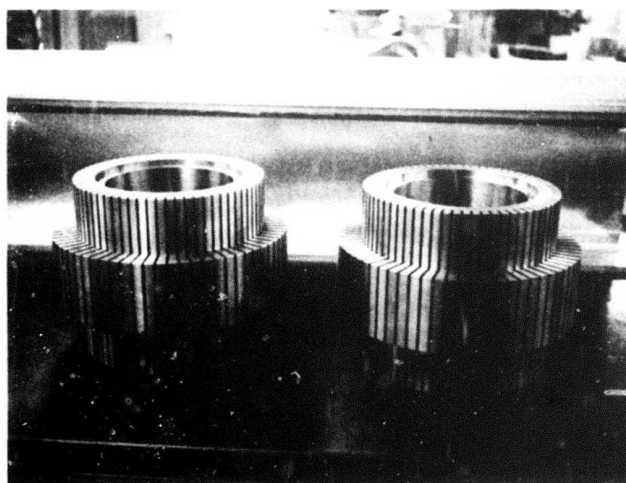
- Stator - All subassembly parts for the stator have been released for machining. The outer stator shell has been rolled and is being finish machined. The inner stator design is complete with the exception of the current collector piping design which will be established on December 15, 1973. Braze mockups for the collector rings and cooling piping braze have been brazed and are being tested.
- Bearing Support End Flanges - The bearing support structure has been released for manufacture. The end flange plates have been semi-finish machined and the bearing brackets are being finish machined.
- Field Excitation Coil - The materials for the excitation coil have been received. The coil detail design will be completed by January 4, 1974.
- Miscellaneous Hardware - The machine coupling, bearings and shaft seal bearing housings have been received.

The SEGMAG fabrication is on schedule with the exception of the field excitation coil which is approximately one week behind schedule. Present projections show that this time can be made up and the fabrication of the field coils will not delay machine testing.

The SEGMAG test stand design has been finalized and construction is to be initiated in mid-December 1973. The test stand motor, gear box, motor control and field exciter motor generator set for the stand have been reviewed. The test stand completion is scheduled for mid-January 1974.



SEGMA Rotor



SEGMA End Modules

Fig. 2-1—SEGMA Components

2.2 GEC GENERATOR

2.2.1 Objectives

The General Electric Company, Ltd., of England has developed an experimental homopolar generator which utilizes a GaIn current collection system. This generator employs an electrochemical purification system to maintain the purity of the liquid metal and avoid the "black powder" problems of previous investigators who used this metal. ARPA has approved purchase of this generator for experimental evaluation under the contract. The machine will be used to provide operating and technical experience with GaIn as a current collector liquid and to supplement the main experimental studies which will be conducted with NaK. This experience is expected to be valuable in broadening the scope of the program beyond the alkali metals. The physical design of the machine and its performance will be investigated thoroughly, and the unit may also be employed as a high current dc source in the current collector test program.

2.2.2 Prior and Related Work

Liquid metal current collection systems have a high potential to function efficiently with long, trouble free life in the face of high electrical current loads and high rotational speeds conceived for homopolar machines of the advanced segmented magnet design.

Based on extensive study, NaK-78 was selected as the best liquid metal for current collectors employed in the SEGMAG machine, and GaIn was selected as the alternate choice.

Since GaIn has been identified as the back-up choice to NaK, the ability to work with and study a functioning GaIn unit is expected to be highly instructional in the general sense and also to shorten any subsequent development effort with GaIn.

Based on an extensive search of the market we have concluded that the GEC machine is the best vehicle to provide the GaIn experience needed for this program. No other liquid metal machine in the world, to our knowledge has operated continuously longer than 40 hrs without maintenance. Therefore, this machine, which has operated up to 1000 hours with no problems, represents a unique development.

2.2.3 Current Progress

The GEC generator was completed in October. A test program was performed on the machine in November to determine machine performance and losses. The test program was witnessed by Westinghouse personnel and consisted of:

- Open circuit test - The machine hydrodynamic and MHD losses were measured as a function of generator speed and field excitation.
- Short circuit tests - The machine I^2R losses were measured as a function of output current at low excitation.
- Motor Mode Tests - The machine was operated as a motor to determine hydrodynamic and MHD losses and to measure machine vibrations when de-coupled from the prime mover.
- Generator Load Tests - The machine was operated with a load bank to determine performance when developing rated power.
- Assembly-Disassembly Test - The machine was assembled and disassembled to familiarize the Westinghouse personnel with machine design and maintenance procedures.

The results of the open circuit tests are shown in Figure 2-2 as a function of speed and field excitation current. Some MHD losses are evident at speeds above 2000 rpm indicating some interaction between the machine field and the GaIn in the current collectors. The data taken during the motor tests are shown in Figure 2-3. The losses determined from the motor tests correlate with those determined from the open circuit tests. The machine vibration readings taken during the motor tests were lower than those obtained during the remaining tests when the generator was driven by the test stand traction motor. This indicates that the majority of the vibration was generated by the test stand drive motor.

The results of the short circuit tests are shown on Figure 2-4. The machine loss is presented as a function of output current at the machine design speed of 3600 rpm. The field excitation used during this test was essentially zero and therefore the losses are an indication of the internal resistance and hydrodynamic losses.

The generator load tests for various machine speeds are shown in Figure 2-5. The maximum current achieved was 32,800 amps at 2200 rpm. The maximum current achieved at 3600 rpm was 24,400 amps. This current level could not be maintained due to excessive heating of the lower current collector. The design current of 16,000 amps was generated at steady state machine conditions.

Two failures were encountered during the test program. The first failure involved the upper radial ball bearing and shaft seals. While running at 3600 rpm, the bearing failed and the machine tests were stopped. Subsequent metallurgical examination of the bearing balls showed a very low hardness. The bearings and seals were replaced and the test was continued with no further bearing or seal problems.

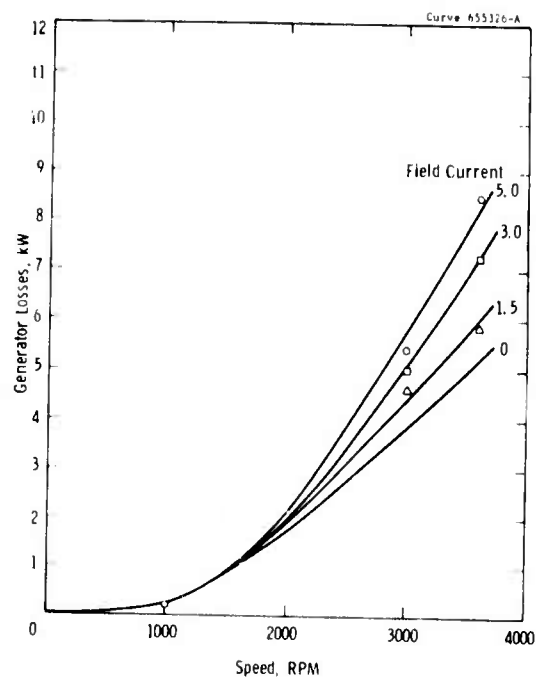


Fig. 2-2-GEC Homopolar Open Circuit Tests

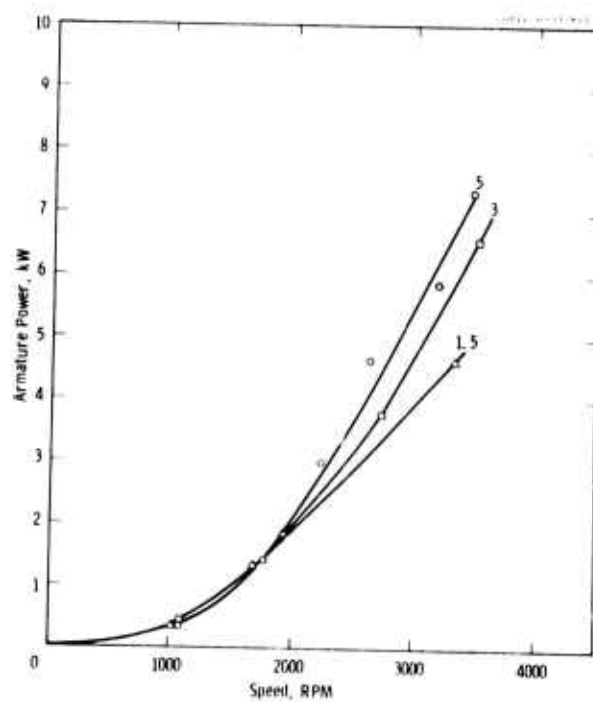


Fig. 2-3-GEC Homopolar Motor Tests

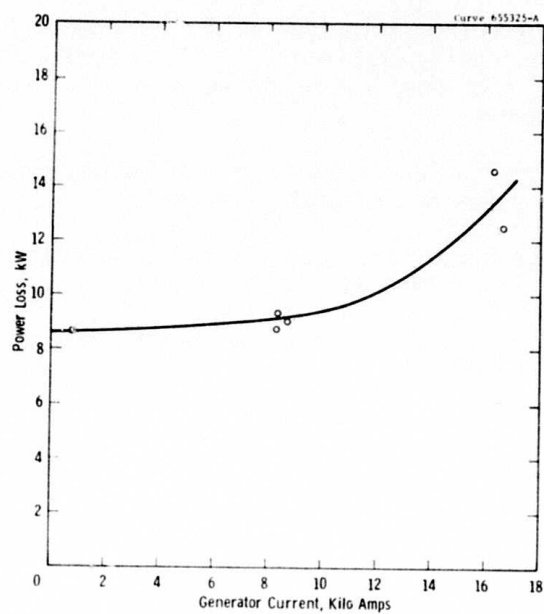


Fig. 2-4-GEC Homopolar Short Circuit Tests

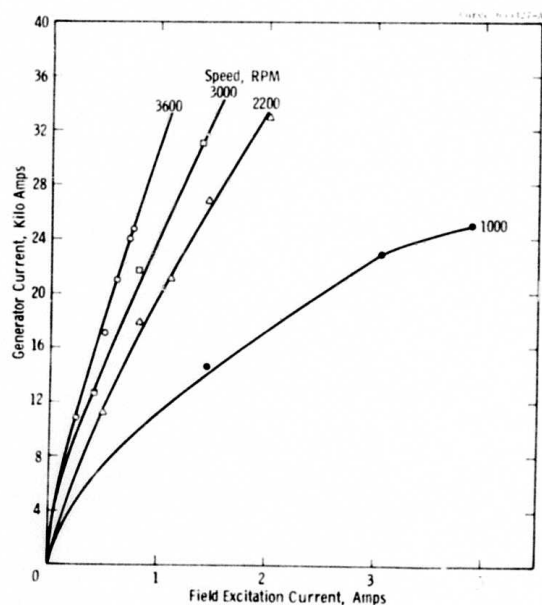


Fig. 2-5-GEC Generator Load Test

The second failure involved GaIn leakage from the machine. The leakage was traced to an improperly compressed "O" ring seal at the lower collector. The "O" ring seal was replaced with no further evidence of leakage from the machine.

At the conclusion of the test program, a preliminary test report was prepared summarizing the entire test program.

The GEC homopolar generator has been shipped to the Westinghouse R&D Center where it will undergo additional testing.

The test stand design has been finalized for the GEC machine. The drive motor has been received. The stand construction will be initiated by early January 1974.

SECTION 3 APPLICATION STUDY

3.0 OBJECTIVES

Review and select promising applications for the segmented magnet homopolar machines and torque converters.

Several of the applications resulting from the Phase II application studies will be reviewed in conjunction with ARPA, and the most useful application will be selected.

3.1 PRIOR AND RELATED WORK

The Semi-Annual Technical Report for Period Ending November 30, 1972 discussed in some detail a number of applications which are potentially feasible. All applications were contingent upon proper solution of the current collection problem. The problem of using liquid metal to transmit simultaneously large quantities of electrical current and heat from the rotating armature must be solved in a reliable and safe fashion to realize these applications. Considerable progress on the hydraulic and dynamic aspects of the current collecting system has been made during Phase II of this study. The potential success of this current collection system provided encouragement to address the applications study.

3.2 CURRENT PROGRESS

During this period the basic advantages of Segmented Magnet machines were reviewed. They are:

1. Very lightweight and low volume.
2. High efficiency.
3. Low excitation power.
4. Low inductance.
5. Low inertia.
6. Potential for low cost.

7. High reliability.

The potential applications of Segmented Magnet machines fall into two general classes, homopolar generators and homopolar torque converters. Utilizing the basic advantages listed above, a list of potential applications of homopolar generators was prepared:

1. High power DC pulsing for lasers and Tokamak Fusion Reactors.
2. High energy transfer as inertial capacitor for fusion reactors.
3. High current for Process Industry.
 - a) Aluminum reduction.
 - b) Chlorine production.
 - c) The electrolysis of water.
 - d) Electro-welding.
4. Electro-plating.
5. Computer power supplies.

A review of the advantages of utilizing Segmented Magnet Homopolar Torque Converters produced the following:

1. Converts high speed-low torque prime mover to low speed-high torque drives.
2. Replaces gears with a low loss electric transmission system.
3. Matches load to any prime mover.
4. High controllability.
 - a) Low excitation power.
 - b) Rapid response.
5. Utilizes the simpler uni-directional prime movers.
6. Full power reverse capability.
7. Ultra-light weight and low volume drive.
8. Variable speed at high efficiency.
9. Low noise level.
10. Compatible with emergency battery power source.

A corresponding list of potential applications was then formulated:

1. Heavy vehicular drive systems.
2. Large antenna drives.
3. Large industrial drives.
4. Ship propulsion systems.
 - a) In-line drives.
 - b) Large submarines.
 - c) Tugboats.
 - d) Small submersibles.
 - e) High speed nuclear navy ships.

SECTION 4

CURRENT COLLECTION SYSTEMS

4.0 OBJECTIVES

The main objectives of this task in Phase II are: (1) to complete construction of a liquid metal current collector test rig with associated support facilities, control, and monitoring equipment for the purpose of carrying on a previously planned experimental program; (2) to initiate and complete an experimental program designed to resolve certain questions or problems anticipated with the application of liquid metal current collectors in homopolar machines; and (3) to establish a viable current collector design suitable for demonstrating feasibility of the SEGMAG homopolar machine concept in a 3000 hp generator.

4.1 PRIOR AND RELATED WORK

During Phase I of the present ARPA contract, a preferred current collector design was identified for powerful homopolar machines. This selection was based on a review study of the complex electromagnetic interactions and forces which will be experienced by functioning collector systems under a variety of operating conditions and liquid metals. The collector design embodies an "unflooded machine gap", with the low density sodium-potassium liquid metal alloy (NaK) confined in narrow circumferential current transfer zones. The liquid metal alloy gallium-indium (GaIn) was selected as an alternative to NaK, especially for homopolar machine applications wherein relatively low speed and high ambient magnetic field operating conditions exist, or in certain situations where liquid metal handling may be considered a problem. The alternative choice of a higher density liquid metal was based on lower calculated power losses when run under the specified operating conditions. Although not as compatible as NaK with most structural and conducting materials, GaIn is quite easy to handle and lends itself to a relatively simple purification process.

Two of the greatest concerns in applying liquid metal current collectors are (a) the magnitude of power losses developed in the fluid due to hydrodynamic, electrodynamic, and joule effects and (b) the confinement of fluid to the current collection zones during all machine operating conditions.

4.1.1 Power Loss Considerations

Although homopolar machines can be shown to develop large output power from a small volume, it is desired that their efficiency be very high. One component of power loss which challenges high machine

efficiency is the current collector loss. Principal types of power loss are (1) ordinary hydrodynamic loss, (2) magnetohydrodynamic (MHD) loss due to a circumferential magnetic force on the liquid, (3) eddy current drag, and (4) ohmic loss due to load current crossing the collector gap. In regard to "unflooded gap" machines, such as SEGMAG, the power losses of the first and fourth type will be small with ordinary hydrodynamic losses dominating. Based on a model selected for the purpose of theoretical analysis, it appears that power loss in the liquid metal due to radial magnetic field effects (third type) can be substantial but lower than hydrodynamic losses. Power loss in the liquid metal associated with axial magnetic field-load current interactions (type two) is expected to be much lower than the radial field induced loss. Considering machines of the SEGMAG type, where the ambient magnetic field in the current collection zone will be very low, the power losses of the second and third type will be small.

4.1.2 Confinement Considerations

The second major concern in the application of liquid metal current collectors is that of confining the fluid to the collection zone. Significant factors are: loss of fluid during low speed and standstill operating conditions because of gravity effects, loss of fluid in the form of aerosols at high speed because of excessive turbidity and surface agitation, and loss of fluid at all speeds because of circulating current and load current effects.

A technical experimental plan was developed to resolve or ascertain the seriousness of concerns associated with the application of liquid metal current collectors such as the above. In particular, the experimental program centers on the resolution of problems associated with the application of collectors in SEGMAG type machines. The technical plan involves experimental investigations to resolve potential problems in regard to (1) injection and withdrawal of liquid metal into and from the current collector, (2) stability of liquid containment in the collector annular gap, (3) retainment of liquid metal chemical integrity in the face of viscous and joulean (ohmic) heating, (4) axial expelling pressure due to load current effects, and (5) development of liquid metal confinement methods.

A test rig capable of evaluating prototypic size liquid metal current collectors under special experimental conditions which simulate those anticipated in a 3000 hp SEGMAG type homopolar generator was designed and its fabrication initiated in early 1973.

4.2 CURRENT PROGRESS

During the current period, data on liquid metal collector power loss, obtained from our previously developed computer program, and other calculated information concerning both power loss and fluid confinement

were reviewed in light of the experimental program parameters. Additionally, preliminary experiments with small current collectors (11.4 and 17.8 cm diameter rotors) were continued to help resolve recognized problems in the area of controlled fluid injection, withdrawal, and confinement. Construction of a large current collector test rig (capable of evaluating 35.6 cm diameter rotor current collectors) with associated support systems, control and monitoring equipment were completed. The experimental program leading to development of a viable liquid metal current collector was initiated. A study of collector hydrodynamic flow characteristics relative to recent experimental results was made. Detailed information concerning the above items is contained in sections 4.2.1 through 4.2.5.

4.2.1 Experimental Program Test Parameters

The selection of test parameters necessary to the evaluation of candidate liquid metal current collectors must involve a knowledge of the anticipated operating and environmental conditions. Such important conditions include ambient magnetic field intensity, electrical load current magnitude, and rotor surface velocity. In addition to these conditions, the collector's performance is also dependent on rotor-stator geometry and certain physical properties of the liquid metal.

Axial Magnetic Field Parameter

In the case of a homopolar generator, the influence of an axial magnetic field on the collector fluid power loss is described by the following basic equation which also contains the effect from ohmic power loss.^{1,2}

$$P_a = \underbrace{\left[\frac{1}{2} f \rho (V_o - V)^2 V_o \right]}_{\text{hydrodynamic}} \underbrace{\left[-B_x J_y V d + \sigma^{-1} d J_y^2 \right]}_{\text{electrodynamic}} A \quad (1)$$

magnetohydrodynamic (MHD)

where: P_a = total power loss per collector, watts.

f = Fanning friction factor.

ρ = fluid density, kg/m³.

V_o = rotor surface velocity at the collector, m/s.

V = liquid metal surface velocity, m/s.

B_x = axial magnetic field, Tesla

J_y = collector load current density, A/m^2 .

D = collector radial gap dimension, m.

σ = electrical conductivity of liquid metal, mhos/m.

A = collector contact area, m^2 .

Results from a computer program developed by Westinghouse to evaluate the above equation for SEGMAG design parameters are presented in Table 4-1. Power loss is shown to increase directly with the collector radial gap dimension and with the axial magnetic field intensity. In the case of a 1.59 mm stator-rotor gap, the MHD collector power loss is shown to increase 10 times as the magnetic field is increased from zero to 2.8 Tesla. Although the ohmic (joulean) power loss magnitude remains constant, it comprises 6.3% of the total collector loss under zero magnetic field conditions and 0.7% when the ambient field is 2.8 Tesla.

The average liquid metal velocity is shown to decrease as the axial magnetic field intensity is increased. At a certain level of magnetic induction, the liquid flow stops, then, with still higher induction levels, reverses in direction. The reverse flow point is reached when the dimensionless collector parameter, k , becomes equal to unity. This collector parameter is a ratio of an MHD body force, which occurs as a result of the axial magnetic field-load current interaction, and a hydrodynamic viscous force, which arises in the fluid due to rotation of the rotor. The MHD body force, F_θ , is obtained from the expression $B_x J_y dA$ and the viscous force by $\frac{1}{2} f \rho (V_0 - V)^2 A$. In the case of a generator, the MHD force tends to pump the liquid metal counter to the direction in which the rotor is driven. If the axial field becomes sufficiently strong, to a point where the collector parameter equals unity, the MHD and the viscous drag forces will become equal and, relative to an observer on the stator, the liquid flow velocity will be reduced to zero. As this operating conditions is approached, the liquid metal will likely "drop out" of the collector, since the inertial constraining force also approaches zero. Thus, even with high speed homopolar generators, if the ambient axial magnetic field becomes critically high, confinement of liquid metal to the collection zone will be a serious problem. This will not happen in the SEGMAG machine because the axial magnetic field in the collector zone is much too low (i.e., about 0.1 Tesla).

Radial Magnetic Field Parameter

Liquid metal current collectors used in homopolar machines may also be subjected to a radial magnetic field. This field induces a

TABLE 4-1

Calculated Power Losses in Current Collector Related to
Axial Magnetic Field and Radial Gap.

Collector Rotor Radius, 0.178 m
Load Current 10^5 amps
Rotor Angular Velocity, 377 rad/sec
Collector Axial Width, 0.0191 m
Collector Current Density, 4.7×10^6 amps/m²

Collector Liquid Metal, NaK-78
Liquid Metal Density, 850 kg/m³
Liquid Elec. Cond., 2.2×10^6 mhos/m
Conducting Area, 0.0213 m²

Collector Radial Gap, d, m	Axial Magnetic Field, B _x , Tesla	Collector Rotor Velocity, V _o , m/s	**Average Liq. Met. Velocity, V, m/s	*Collector Parameter, k	Power Losses, P _a kW		
					MHD	Ohmic	Total
1.59×10^{-3}	0	67.0	33.5	0	5.02	0.34	5.36
"	0.4	"	24.0	0.28	6.22	"	6.56
"	0.8	"	14.5	0.57	9.88	"	10.22
"	1.2	"	5.0	0.85	15.89	"	16.23
"	1.6	"	-4.1	1.13	23.98	"	24.32
"	2.0	"	-11.7	1.41	32.67	"	33.01
"	2.4	"	-18.3	1.70	41.86	"	42.20
"	2.8	"	-24.1	1.98	51.42	"	51.76
7.62×10^{-4}	0	67.0	33.5	0	5.08	0.17	5.25
"	0.4	"	30.4	0.12	5.85	"	6.02
"	0.8	"	26.0	0.24	6.77	"	6.94
"	1.2	"	21.7	0.36	8.22	"	8.39
"	1.6	"	17.4	0.48	10.17	"	10.34
"	2.0	"	13.3	0.60	12.61	"	12.78
"	2.4	"	9.2	0.72	15.54	"	15.71
"	2.8	"	5.1	0.85	18.95	"	19.12

$$*k = \frac{2 B_x J_y d}{f \rho V^2}$$

**Calculations are for a generator, with the magnetic excitation source held by the stationary part of the machine.

potential gradient along the moving collector face, thereby producing a current distribution within the liquid metal medium between the stationary and moving faces. These eddy currents, in turn, produce a steady state power loss within the liquid metal, even under "no load" conditions with no external current flowing through the collector. Analyses have previously been made to provide a basis for estimating power losses due to the radial field effects.^{1,2} In these works, the effect of fluid velocity interaction with the magnetic field was neglected. In recent work, the effect of fluid motion on the induced eddy currents within the collector gap was taken into account.³ The latter analysis indicates that fluid motion has little effect upon the total eddy current losses (approximately 3% reduction). The derived equation from this latest work, which allows prediction of power loss in the collector due to a radial magnetic field, is shown below.

$$P_r = \frac{\pi \sigma}{\sigma} V_0^2 B_y^2 r \left(wd + \frac{w^3}{d} \right) \quad (2)$$

Where the terms not previously identified are:

P_r = total power loss per collector, watts

B_y = radial magnetic field, Tesla

r = radius of rotor, m

w = width of collector, m

Calculated power losses attributed to radial field effects for the same SEGMAG collector design used previously in the axial field evaluation are shown in Table 4-2. Power loss is shown to increase inversely with the collector radial gap dimension and directly with the radial magnetic field intensity. Compared to the axial magnetic field case, relatively low radial field intensities cause very high power loss. This contrast is shown in Figure 4-1. If the model chosen is correct the achievable efficiency of machines which impose high radial fields on the current collectors should be of great concern. Fortunately, in the case of SEGMAG type machines, the current collector ambient magnetic field will be very low (estimated to be 0.03 Tesla radial, 0.10 Tesla axial). The additional MHD power losses will be somewhat less than the ordinary hydrodynamic and ohmic power losses in SEGMAG machines.

Load Current Parameter

Since losses due to axial magnetic fields will be extremely small in the SEGMAG demonstration machine, there is no need for either a high electrical load current (10^5 amperes) or an axial magnetic field in the experimental test program to evaluate the associated small MHD effect.

TABLE 4-2
Calculated Power Loss in Current Collector Related to Radial
Magnetic Field and Radial Gap

Collector Rotor Radius, 0.178 m Collector Liquid Metal, NaK-78
Rotor Angular Velocity, 377 rad/s Liquid Elec. Cond., 2.2×10^6 mhos/m
Rotor Width, 1.91×10^{-2} m

Collector Radial Gap, d, m	Radial Magnetic Field, B _r , Tesla	Collector Rotor Velocity, V _o , m/s	Power Loss, P _r , kW
1.59×10^{-3}	0	67.0	0
"	0.02	"	1.61
"	0.04	"	6.46
"	0.06	"	14.53
"	0.08	"	25.84
"	0.10	"	40.37
"	0.12	"	58.14
"	0.14	"	79.13
7.62×10^{-4}	0	67.0	0
"	0.02	"	3.37
"	0.04	"	13.48
"	0.06	"	30.33
"	0.08	"	53.91
"	0.10	"	84.24
"	0.12	"	121.31
"	0.14	"	165.11

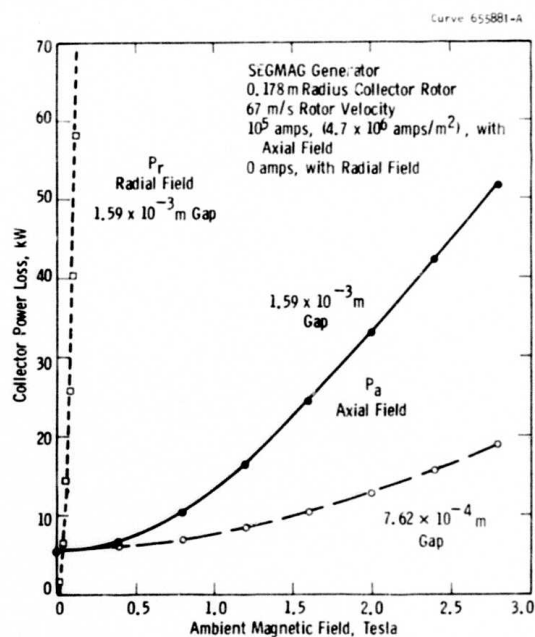


Fig. 4-1—Liquid metal (NaK-78) current collector power losses from
magnetic field effects

It is only necessary to evaluate the ordinary hydrodynamic effect and the radial field effect. In regard to this latter effect, an electromagnet was designed to provide magnetic induction levels to 0.1 Tesla in the test rig current collectors. Although this maximum test induction is three times the radial field level anticipated in the SEGMAG machine, it will permit a positive check to be made on the predictive loss equation (2).

Here, again, there is no test requirement for a high electrical load current to check the radial magnetic field effect. The radial field induces a voltage along the rotating collector face, thereby producing, by itself, a very large circulating (eddy) current within the liquid metal. It is estimated that eddy currents greater in magnitude than the normal load current will be circulated in the liquid metal. The level of these currents can be estimated from changes in rotor drag torque as the field is switched on or off. Alternatively, the eddy current magnitude can be estimated from measurements of voltage drop across the collector stator width. This technique is supported by a recent analytical study which revealed that about 96% of the eddy current will flow across the liquid metal into the stationary collector, with 4% flowing entirely within the gap region. The employment of a radial magnetic field to create high electrical current in the collector can be used to check the effect of combined viscous and joulean (ohmic) heating on the liquid metal's chemical integrity.

Rotor Surface Velocity Parameter

As the ambient magnetic field approaches zero in the current collection zone, the ordinary liquid metal viscous power loss can be shown to vary approximately as the cube of the rotor surface velocity.

$$P_{vis} = \frac{f \rho V_o^3}{8} A \quad (3)$$

Since only very low level magnetic fields will be encountered in the SEGMAG machine, it is desirable to evaluate candidate current collectors at speeds typical for the demonstration generator. The test rig is capable of being driven from zero to about 70 rps. Both viscous power loss characteristics and liquid metal confinement capabilities can be evaluated for the candidate current collectors over this wide range of rotor speeds.

4.2.2 Preliminary Experiments With Small Test Rigs

Numerous tests, covering hundreds of hours, were conducted during the period on liquid metal current collectors with 11.4 and 17.8 cm diameter disk rotors. A summary of the small collector designs evaluated is

shown in Table 4-3. All collector designs included copper rotors. Plastic stators were used in most cases to permit direct observation of fluid flow in the annulus between the rotor and the stator. Electric probes were embedded in some of the plastic stators to monitor fluid flow continuity in the annulus and to provide a means for estimating the electrical contact resistance. Liquid metal feed techniques included batch, sump weir from the side, and direct tangential. Collector sealing against NaK loss varied from simple sump covers to modified or partial labyrinth seals.

The significant experimental results arising from testing the small model current collectors are given below.

- Liquid metal (NaK) can be drawn, from a pool at the bottom of a collector, into the annular gap of the collector and held there by centrifugal (inertia) force.
- Liquid NaK can be continuously withdrawn from, filtered, and returned to the annular gap while the collector is in its operating mode.
- Feeding fresh NaK into the collector annulus at the free surface of the residing NaK, by way of an axially adjacent open sump-weir arrangement, results in considerable loss of NaK. This occurs because NaK is circulated in the sump through fluid coupling with NaK in the annular gap. Because insufficient velocity is imparted to the sump NaK, it is expelled from the collector by sloshing action, etc., especially on start up.
- Use of a cover over the sump prevents gross loss of NaK associated with fluid coupling effects. Expulsion of NaK by sloshing and splashing actions is prevented by the sump cover seal. Injection of NaK into the collector annulus is accomplished through a sluice opening provided.
- Liquid metal in the radial gap and for short radial extents along the axial flat sides of a collector rotor may typically possess an average velocity hundreds of times greater than that of the inflowing fluid from the inlet sump. Effects of the transition from relatively low to high velocity will enhance surface instability and this is thought to be a major cause of aerosol formation.
- Tangential feeding of NaK directly into the collector annulus has a less disturbing effect on the flow and results in less fluid loss from the collector than when fed by the side sump-weir technique.

TABLE 4-3
Summary of Small Current Collector Designs

I. 11.4 cm Diameter Rotor (13.1 m/s speed, 1.24 mm radial gap)

Materials		Rotor End Shape	Liquid Metal Feed	Collector Seal	NaK Loss Rate, cc/min	Approx. Operating Time, hr
Rotor	Stator					
Cu	Cu	Tapered (60°)	Batch Tangential	No	Small	500
Cu	Plastic	"	Batch Sump-Weir	No	2-4	10
Cu	Plastic	"	Sump-Weir	Sump Cover	1	100
Cu	Cu	Flat	Tangential	Deflector- Channel	nil	600

II. 17.8 cm Diameter Rotor (32.9 m/s speed, 1.60 mm radial gap)

Cu	Plastic	Flat	Sump-Weir	Sump Cover	~3	25
Cu	Plastic	"	"	Sump Cover- Deflector Channel	1.5	50
Cu	Cu	"	Sump-Weir (Asymmetrical)	Sump Cover- Slinger- Channel	1	30

- A significant reduction in loss of liquid metal from the collector in the form of aerosol or droplets can be achieved by employing a deflector surface on the rotor and a concentric annular groove channel in the stator. The preferred shape for the channel trap is a deep groove with straight, rather than curved, side walls.
- A 6.35 mm diameter effluent drain line will permit through-flow rates of NaK-78 up to $13.3 \text{ cm}^3/\text{s}$ to be sustained, even when the rotor is stopped. No overflowing of the exit sump occurs. The drain line diameter does not represent a limiting size for handling $13.3 \text{ cm}^3/\text{s}$, but that flow rate was the highest tried during the experiment.
- With the 6.35 mm diameter effluent drain tube, and 1.59 mm axial clearance between rotor and stator, the rotor could be slowed down gradually to standstill without spillage of NaK from the collector. Near zero speed the NaK fluid quietly flowed circumferentially each way from the top to the bottom of the collector annulus and mixed with the incoming and outgoing NaK.
- The continuity of fluid flow in the collector gap is improved with increasing inlet flow rates. Although a flow rate of $0.8 \text{ cm}^3/\text{s}$ was adequate to cause high electrical conductivity, hydrodynamic power loss measurements reveal the collector gap was only partially (33-50%) filled. When the inlet flow rate was increased to $7.5 \text{ cm}^3/\text{s}$ electrical conductivity was very stable and power loss data indicate the gap was completely filled with NaK.
- During operation with low inlet flow rates, observations of the NaK flow in the collector annular gap reveal that the fluid may be broken up by gas bubbles or streamers. Results of electrical conductivity measurements reveal that the gas volumes may be 1.59 to 8.47 mm in circumferential length.
- Results of electrical conductivity measurements, made between two 1.59 mm diameter copper probes located 120° apart along the stator circumference and just penetrating into the annular gap fluid, reveal that contact resistance is nil. Consequently, excellent "electrical wetting" occurs between NaK and copper surfaces and the volume resistance of NaK will govern the joulean heating when electrical currents are transferred across the rotor-stator collector gap.

4.2.3 Large Test Rig

Fabrication and assembly of the large (35.6 cm diameter rotor) liquid metal current collector test rig, associated cover gas and NaK supply systems, and control and instrumentation equipment were completed during the period. The rig is capable of receiving current collectors of the same size as those to be used in the 3000 hp SEGMAG demonstration machine. Consequently, scaling of results will not be required for that application. Features of the overall test stand which were incorporated to meet needs of the experimental test plan are discussed in the previous semi-annual technical report. An overall view of the current collector test stand is shown in Figure 4-2.

The test rig was subjected to a 20% overspeed run prior to its installation in the glove box. This run was made to check the ability of the rotor to withstand the test speed rotational forces. After it was installed in the glove box. This run was made to check the ability of the rotor to withstand the test speed rotational forces. After it was installed in the glove box, the rig vibration characteristic was observed over the normal speed range. Acceptably smooth running was found, with a maximum vibration amplitude of 0.036 mm near 19 rps.

4.2.4 Experiments with Large Test Rig

Numerous tests, totaling over 200 hours of running time, were conducted during the period on liquid metal current collectors with 35.6 cm diameter disk rotors. A summary of the collector designs evaluated is shown in Table 4-4. The first five designs, α through ϵ , were fabricated and evaluated during the period. The latter two designs are being readied for evaluation.

The current collector experiments performed to date covered a wide range of speeds (to 60 rps), with no magnetic field effects. Since the SEGMAG machine will impose very low axial magnetic fields on the collectors, one needs to consider mainly the viscous power loss due to ordinary hydrodynamic effects. Later, however, the effect of radial magnetic fields will be evaluated.

The goal of these experiments was to obtain a viable current collector for subsequent testing under possibly more severe operating conditions. In regard to that goal, good results have been obtained with current collector design δ , and excellent results with design ϵ . The latter collector has been run at speeds to 60 rps for over 100 hours, during which time complete filling of the gap was achieved and loss of NaK from the collection zone was nil. Complete filling of the collector annulus with liquid metal was evidenced from electrical probe continuity indications, pressure tap gauge readings, and viscous rotor drag torque measurements.

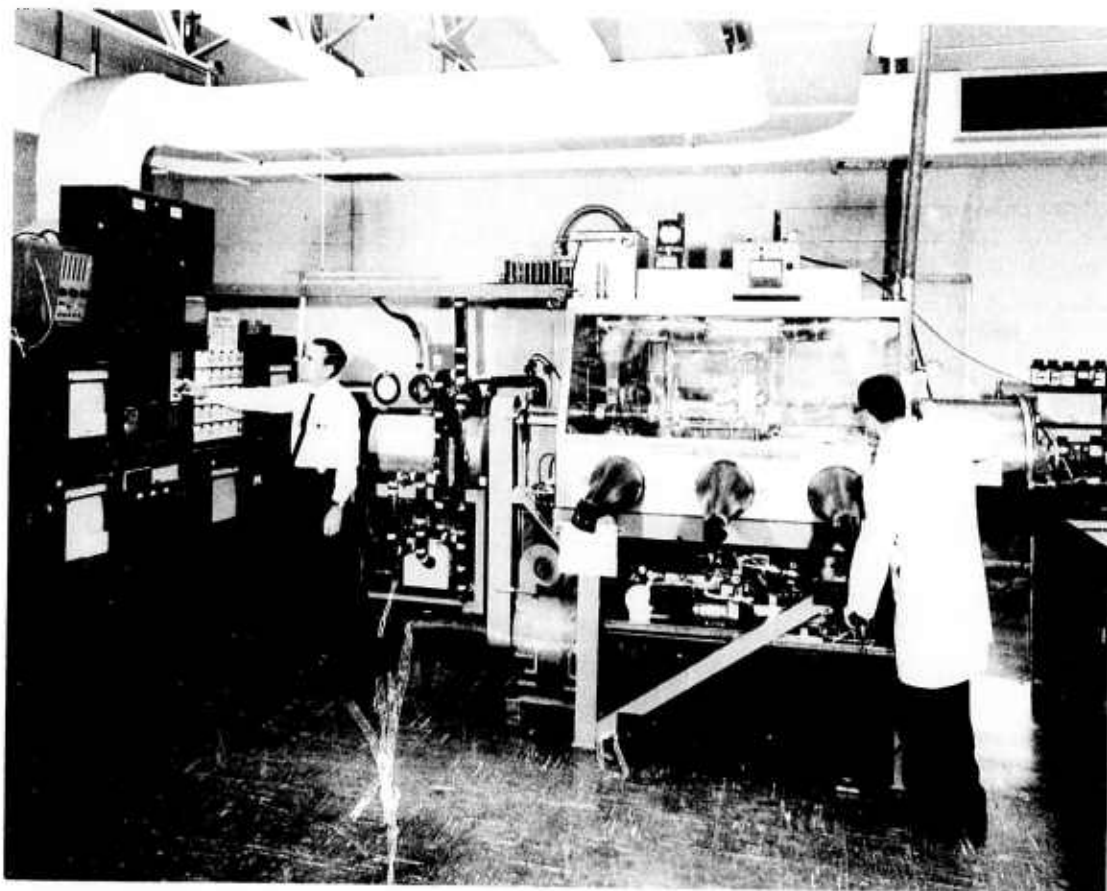


Fig. 4-2—Liquid metal current collector test stand

TABLE 4-4

SUMMARY OF PROTOTYPIC SIZE COLLECTOR DESIGNS
(35.6 cm Diameter Rotor, Speeds to 67 m/s, 1.59 mm gap)

Collector Design	Rotor End Shape	Liquid Metal Feed	Collector Seal	Liquid Metal Drain
α	Flat	Sump-Weir	Face	Weir-Sump
β	Tapered	Sump-Weir	Face	Weir-Sump
γ	Flat	Direct-Radial	Multiple Groove	Side Interceptors
δ	Tapered	Direct-Radial	Multiple Groove	Inward-Displaced Side Interceptors
ϵ	Flat	Direct Tangential	Multiple Groove	Inward-Displaced Side Interceptors
<hr/>				
ξ	Flat (with flow constrictors)	Direct Tangential	Multiple Groove	Inward-Displaced Side Interceptors
η	Tapered	Direct-Tangential	Multiple Groove	Inward-Displaced Side Interceptors

The viscous torque-NaK flow characteristics for collector ϵ are shown in Figure 4-3. This family of curves reveals that, with increasing NaK inlet flow rate, a limiting maximum torque level is approached. The limiting torque level is different for each speed, becoming higher as the speed is increased. Based on electrical continuity measurements, complete filling of the gap occurs at low inlet flow rates, near the starting knee of the curves. Of significance is that this collector is capable of satisfactory operation over a wide range of NaK inlet flow rates, from 0.8 to at least 13.3 cm³/s.

Computations of viscous power loss-speed characteristics for collector design ϵ were made using the experimentally determined torque data. The expression employed for making the computations and which relates power loss and torque is

$$P_{vis} = \omega T, \text{ watts.} \quad (4)$$

where: ω = angular velocity of the rotor, rad/s

T = viscous drag torque, N-m

Torque values used in the computations were selected from the test conditions wherein 6.7 cm³/s NaK inlet flow was employed. The power loss values, determined from these experimental torque measurements, are plotted as a function of rotor speed in Figure 4-4.

The power loss due to viscous shear in the liquid may be calculated from the predictive equation (3). Results of such calculations, are shown by the dashed curve in Figure 4-4. Uncertainty in the values of friction factor, f , and contact area, A , used in the calculations undoubtedly contribute to the imperfect curve matching shown. Fanning friction factor values were determined for each speed from Reynolds number calculations (see Section 4.3.5) and the Moody diagram. The predictive model assumes that the average fluid velocity is one-half the rotor velocity. Slight differences in this assumption from the actual fluid velocity will contribute to significant error, since that factor is raised to the third power. Even so, there is good agreement between the experimental and predictive results.

During the course of experimental work, current collector performance was found to be critically dependent on temperature. This temperature sensitivity characteristic is illustrated in Figure 4-5. Good performance was observed, in terms of gap filling and confinement of NaK to the collector, if operation occurred at temperatures above a critical level for each speed. Operation below the critical temperature line caused an adverse effect on collector performance. Although an experimental solution to the liquid metal current collector problem seems to be achieved by operating above the critical temperature, an explanation

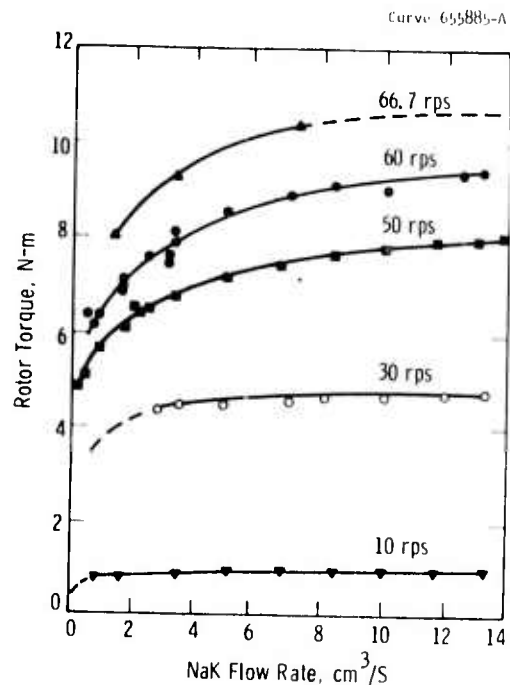


Fig. 4-3—Viscous torque - NaK flow characteristics for rotating disk collector ϵ

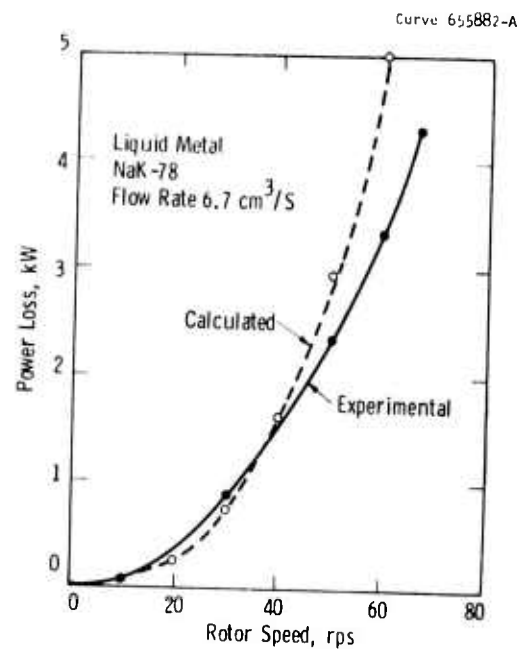


Fig. 4-4—Comparison of experimentally determined and calculated viscous power loss-speed characteristics for rotating disk collector ϵ

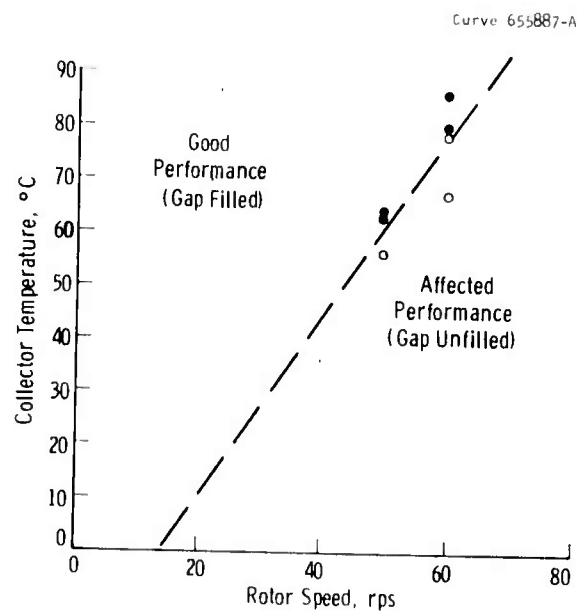


Fig. 4-5—Critical performance-temperature curve for rotating disk collector ϵ

for the complex fluidynamic flow phenomenon in the annulus is not clearly understood at this time. It is interesting to note that the viscosity of NaK changes about 25% in the temperature range of interest. The implications of this physical property change, as well as other factors are considered in Section 4.3.5.

An extended continuous run was made with current collector ϵ over a period of 76 hours. Operating conditions which were held constant throughout the period include rotor speed (60 rps), collector temperature ($38^\circ\text{C} \pm 2^\circ\text{C}$) and NaK inlet flow rate ($3.3 \text{ cm}^3/\text{s}$). The following important collector performance responses also held constant during the test period: rotor viscous torque (7.9 N/m), and radial gap liquid pressure ($2.07 \times 10^4 \text{ N/m}^2$), representative of a completely filled annulus. No loss of liquid NaK was noted during the period, indicating that the collector seals performed in an excellent manner. An extremely thin dust film settled out on surfaces near the collector. It is estimated that the total accumulation of this debris was $< 0.3 \text{ cm}^3$. Based on the NaK inlet flow rate, this amount of debris represents a loss rate of less than one part in three million. An analysis of the liquid metal composition before and after the run showed no detectable change in the eutectic composition as a result of the viscous working. A photograph reproduction of the test collector in the glove box following the 76 hour run is shown in Figure 4-6.

4.2.5 Fluid Flow Considerations

As previously mentioned, a critical temperature level appears to exist for each rotor speed above which a significantly more desirable fluid flow characteristic occurs in the collector gap annulus (see Figure 4-5). It is of interest to consider this phenomenon in terms of the dimensionless Reynolds number, which relates the ratio between inertia and viscosity fluid forces.⁴ Since viscosity is also temperature dependent, seeking a correlation between the Reynolds number and the collector fluid flow characteristics is justified.

$$N_R = \frac{v\ell}{\nu} \quad (5)$$

where: N_R = Reynolds number

v = average fluid velocity, m/s

ℓ = characteristic dimension, taken here to be four times the area of flow cross-section divided by the wetted perimeter, m

ν = kinematic viscosity of the fluid, m^2/s .

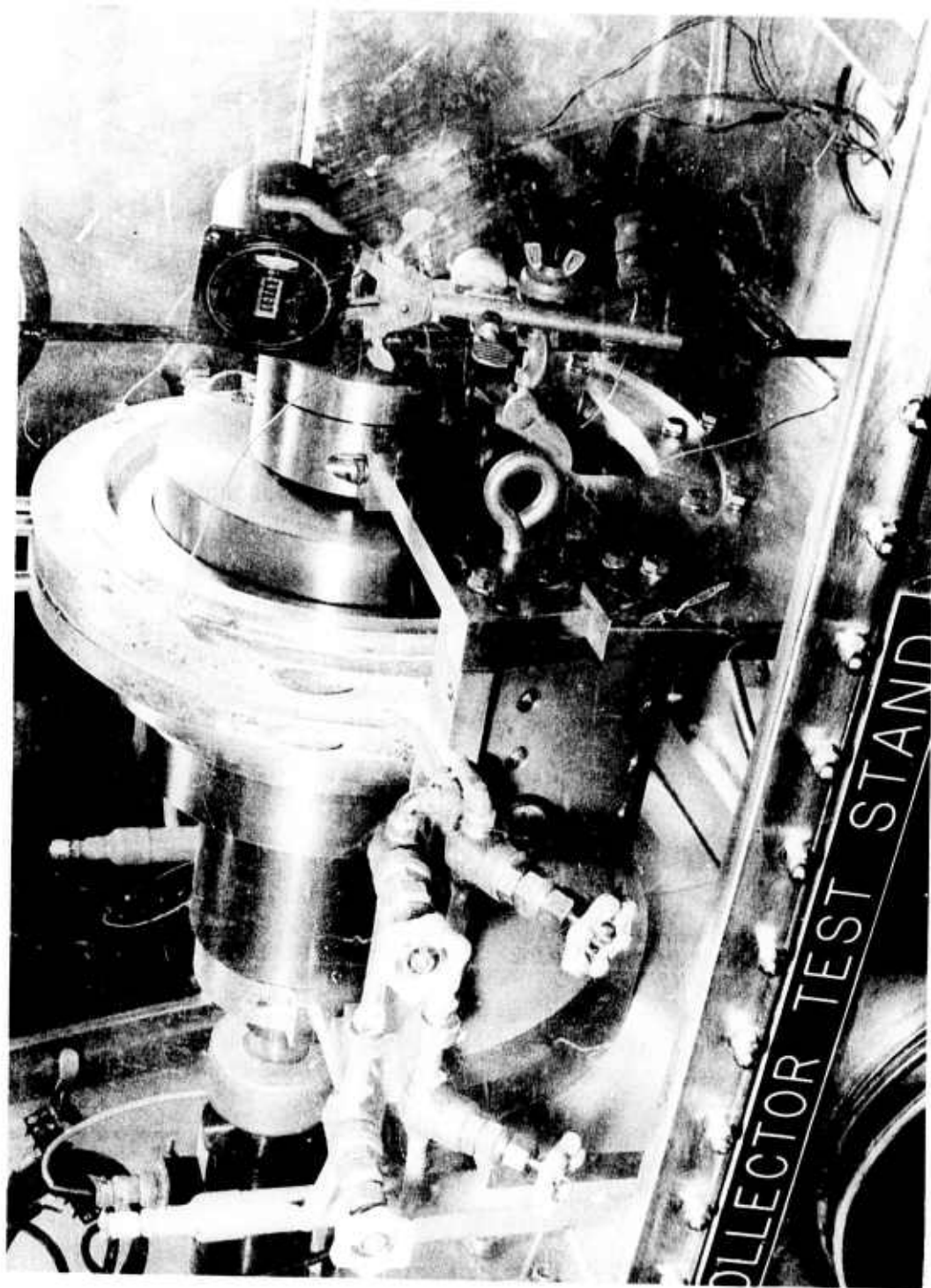


Fig. 4-6--Test collector ϵ after 76-hour run in glove box

The average fluid velocity will be taken as half the rotor velocity. This assumption is made for conditions wherein equally smooth rotor and stator walls exist and where no or very little magnetic field-load current interaction occurs in the liquid metal. The latter is typical of the experimental condition which was imposed by the test rig and subsequently to be imposed on similar current collectors by the SEGMAG demonstration generator, respectively. Assuming NaK completely fills the rotor-stator radial annulus, the characteristic dimension may be taken as twice the radial gap. Then

$$N_R = \frac{(\frac{1}{2} \omega r)(2d)}{v} = \frac{\omega r d}{v} \quad (6)$$

Where: ω = angular velocity of the rotor, rad/s

r = rotor radius, m

d = extent of rotor-stator radial gap, m

Appropriate information needed to calculate the Reynolds number for the current collector critical speed-temperature conditions is contained in Table 4-5.

Calculated values of the Reynolds number corresponding to the given rotor speed-critical temperature conditions and normalized values of temperature and viscosity are shown in Table 4-6.

Based on the large Reynolds number shown in Table 4-6, inertial rather than viscous force appears to be the dominant one which controls the fluid flow characteristics.

In the case of fluid flow through circular pipes, the conditions below which turbulence entering the flow will be damped out by viscosity is defined by Reynolds numbers in the range 2000-4000. Since the critical Reynolds number for given fluid applications depends on geometrical shape of the flow system, the above value range is probably not applicable for the current collector configuration.

Fluid flow in the annulus between two long concentric cylinders, wherein the inner cylinder rotates, has been studied by others.⁵ Under certain conditions, loss of stability is made manifest by the appearance of vortices (called Taylor vortices) in the meridian plane, the circulation of which alternates from one to the next. The velocity at which the vortices begin to be formed, if the radial gap to inner cylinder radius ratio is small, can be calculated from the equation

$$2 \left[\log \frac{r_2 \omega (r_2 - r_1)}{v} \right] + \log \frac{r_2 - r_1}{r_1} = 3.232 \quad (7)$$

where: r_1 = radius of rotating inner cylinder

r_2 = radius of stationary outer concentric cylinder.

TABLE 4-5
Data for Critical Reynolds Number Calculations

Rotor Speed, rps	*Collector Temp., °C	Physical Properties for NaK-78		
		Mass Density, ρ , kg/m ³	Dynamic Viscosity, μ , N-sec/m ²	Kinematic Viscosity, ν , m ² /sec
10	-6	875.58	8.187×10^{-4}	9.350×10^{-7}
20	10	870.43	7.325×10^{-4}	8.415×10^{-7}
30	27	865.79	6.511×10^{-4}	7.520×10^{-7}
40	44	862.70	5.985×10^{-4}	6.938×10^{-7}
50	61	861.16	5.506×10^{-4}	6.394×10^{-7}
60	78	854.46	5.075×10^{-4}	5.939×10^{-7}

*Experimentally established critical performance temperatures (Fig. 4-5) for collector with 17.8 cm radius rotor and 1.59 mm radial gap.

TABLE 4-6
Calculated Reynolds Number for Critical Flow Conditions

Rotor Speed, rps	Critical Temp., °K	Reynolds Number, N_R	Normalized Quantities	
			Absolute Temp.	Reciprocal Kinematic Viscosity
0	267	1.90×10^4	0.76	0.64
20	283	4.22×10^4	0.81	0.71
30	300	7.08×10^4	0.86	0.79
40	317	10.22×10^4	0.90	0.86
50	334	13.87×10^4	0.95	0.93
60	351	17.96×10^4	1.00	1.00

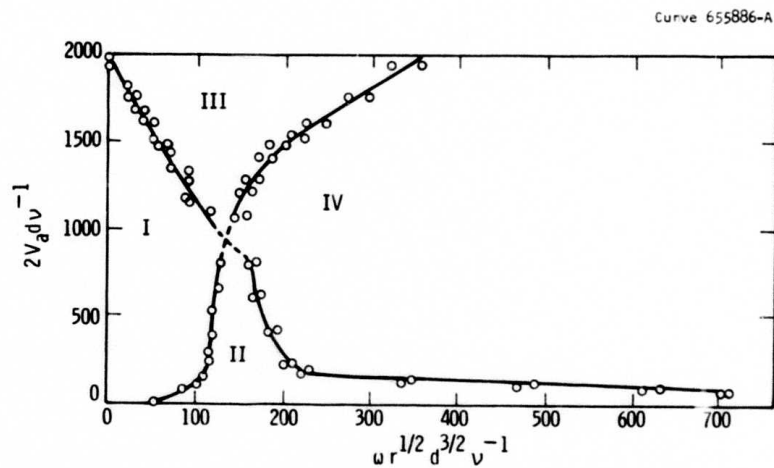


Fig. 4-7—Distribution of the states of flow as functions of the Reynolds number $2V_d \nu^{-1}$ and the Taylor number $\omega r^{1/2} d^{3/2} \nu^{-1}$; (I) zone of purely laminar flow; (II) laminar flow with Taylor vortices; (III) purely turbulent flow; (IV) turbulent flow with Taylor vorticity (according to Kaye and Elqar)

The form of the above equation can be changed to

$$\frac{r_1^{1/2}(r_2-r_1)^{3/2}\omega}{\nu} = 41.3 \quad (8)$$

Loss of stability of the laminar flow is characterized by the dimensionless number $r_1^{1/2}d^{3/2}\omega\nu^{-1}$, which is named the Taylor number after G. I. Taylor. With further changes in form, the above equation can be written

$$\left(\frac{\omega r_1 d}{\nu}\right) \frac{d^{1/2}}{r_1^{1/2}} = 41.3, \text{ or} \quad (9)$$

$$N_{R_{crit}} = 41.3 \sqrt{\frac{r_1}{d}}.$$

This equation permits calculation of the critical Reynolds number, above which Taylor vortices begin to be formed in the flowing fluid. The critical Reynolds number for a prototypic size current collector is 437, based on selected values of 17.8 and 0.159 cm for r_1 and d , respectively. From the significantly greater Reynolds numbers determined previously and shown in Table 4-6, it appears certain that the liquid flow regime of the rotating disk collector will include Taylor vortices.

Work by others reveals that the state of flow in the annular gap is characterized by two numbers: the Reynolds number for the axial flow $2\nu\omega d^{-1}$ and the Taylor number $r_1^{1/2}d^{3/2}\omega\nu^{-1}$. They showed that four states of flow exist: 1) pure laminar flow; 2) laminar flow with Taylor vortices; 3) pure turbulent flow; 4) turbulent flow with vorticity. The characteristic distribution of these regions of flow as functions of the Reynold and Taylor numbers is given in Figure 4-7. Based on the distributions shown and a calculated Taylor number of 16,971 for the prototypic size collector when running at a speed of 60 rps, the liquid flow regime will possess vorticity and may be either laminar or turbulent, region II or IV. The possible transition from one flow region to the other is dependent on the Reynolds number associated with fluid flow in the axial direction.

Near critical operating conditions, if the above is true, slight changes in the axial flow velocity or fluid viscosity (temperature) can cause a dramatic "jump" in the state of flow. Under certain controlled operating conditions in the laboratory, rather sudden dramatic changes in the fluid flow character in prototypic size collectors have been initiated by small changes in either the NaK inlet flow rate or its temperature. For example, an increase in the fluid inlet flow rate

(increased axial velocity) or an increase in its temperature (reduced viscosity) caused a previously unfilled collector annulus to be filled. Such changes in axial flow velocity and, or, fluid viscosity would result in a higher Reynolds number, suggesting a possible shift in the flow region from laminar to turbulent, see Figure 4-7.

As previously mentioned, the Reynolds number is a ratio of the inertia and viscosity forces. The magnitude of computed Reynolds numbers reported in Table 4-6 are significantly greater than unity, indicating that inertia is the controlling force.

There are other forces in addition to inertia and viscosity which may act on the collector liquid metal and influence its flow. Three such forces are those of pressure, gravity, and surface tension. Ratios of the forces are helpful in determining in a quantitative manner the relative extent to which each force acts to affect fluid flow. Such force ratios are usually named for the experimenters who first derived and used them.

The Weber number is a ratio of the inertia and surface tension forces. This ratio indicates which of the two forces is most effective in confining liquid metal to the collector gap.

$$N_W = \frac{\rho d v^2}{\gamma} \quad (10)$$

The Froude number is a ratio of the inertia and gravity forces. This ratio is of special interest in slow speed (motor) applications where "drop out" of liquid metal may result from gravity (g) effects.

$$N_F = \frac{v^2}{2rg} \quad (11)$$

The "MHD" number represents a ratio of inertia force to the load current axial-directed body pressure force. This ratio provides an estimate of how well the liquid will resist axial expulsion from the collector.

$$N_{MHD} = \frac{\rho v^2}{(2n-1)6.28 \times 10^{-7} I_p^2}$$

The Bond number represents the ratio of gravity to surface tension forces. This ratio, as the Froude ratio, is of interest in regard to liquid metal confinement during conditions of low speed operation.

$$N_B = \frac{\rho 2rdg}{\gamma} \quad (13)$$

The following assigned parametric values are typical of those anticipated for the SEGMAG generator application.

- $\rho = 854.5 \text{ kg/m}^3$, mass density of NaK-78 fluid.
 $N = 60 \text{ rps}$, rotational speed of rotor.
 $r = 0.178 \text{ m}$, radius of rotor.
 $\omega = 189 \text{ rad/s}$, angular velocity of fluid.
 $v = 33.5 \text{ m/s}$, velocity of fluid.
 $n = 1$, number of electric circuits at each collector site.
 $I_p = 71,611 \text{ amps/m}$, electric load current per unit of collector periphery.
 $d = 1.59 \times 10^{-3} \text{ m}$, radial gap of collector
 $\gamma = 0.115 \text{ N/m}$, surface tension of NaK-78.
 $g = 9.81 \text{ m/s}^2$, gravity constant.

A summary of the computed fluid flow characterizing numbers is shown in Table 4-7.

TABLE 4-7
Dimensionless Fluid Flow Characterizing Numbers

<u>Characteristic Number</u>	<u>Fluid Force Ratio</u>	<u>Ratio Value</u>	<u>Controlling Force</u>
N_R (Reynold)	Inertia/Viscosity	179,600	Inertia
N_w (Weber)	Inertia/Surface Tension	13,258	Inertia
N_F (Froude)	Inertia/Gravity	321	Inertia
N_{MHD} (Elec. Load)	Inertia/Load Current	298	Inertia
N_B (Bond)	Gravity/Surface Tension	41	Gravity

Based on the above tabulated results, fluid flow in the collector gap will be significantly influenced or controlled by the inertia force. For generator applications, the inertia force will work to confine liquid metal to the collector against gravity and load current expelling effects. For motor applications (low and zero speed conditions) the surface tension force will not be sufficient to prevent "drop out" of NaK-78 due to the force of gravity. A different collector design or concept will be required for low speed running conditions.

4.3 REFERENCES

1. Mole, C.J., et al, Design and Development of a Segmented Magnet Homopolar Torque Converter, Westinghouse Research Report 73-8B6-LIQMT-R1, March 12, 1973.
2. Rhodenizer, R.L., Development of Solid and/or Liquid Metal Collectors for Acyclic Machines, Final Report for task 1, 2, and 3, Navy Ship Systems Command Report, Contract No. N00024-68-C-5414, Feb. 27, 1970.
3. Hummert, G.T., Calculation of Eddy Losses in Liquid Metal Current Collectors, Westinghouse Research Memo 73-8G1-LIQMT-M1, Nov. 20, 1973.
4. Vennard, J.K., Fluid Mechanics, John Wiley and Sons, Inc., 1948, pp. 142-148.
5. Dorfman, L.A., Hydrodynamic Resistance and the Heat Loss of Rotating Solids, Oliver and Boyd, 1963, pp. 163-170.
6. Kaye, J., and Elgar, E.C., Modes of Adiabatic and Diabatic Fluid Flow in an Annulus with an Inner Rotating Cylinder, Trans. ASME, 80, 1958, pp. 753-765.

SECTION 5

LIQUID METAL SUPPORT SYSTEMS

5.0 OBJECTIVES

The objectives of this task during Phase II are: (1) to investigate the compatibility of candidate machine materials with NaK and GaIn, as well as with potential decontamination solutions; (2) to perform literature, analytical, and experimental studies for the purpose of identifying suitable materials and suggesting alternate choices where necessary; (3) to design, fabricate, and test the liquid metal loop and cover gas systems that will be required in the SEGMAG generator; and (4) to establish the operating parameters and interactive responses of these systems.

5.1 PRIOR AND RELATED WORK

Prior and related work are described in the previous semi-annual technical reports^{1,2} of this subject contract. Related work exists in a program being conducted at the Naval Ships R&D Center and in contracts let by the Navy to Garrett AiResearch and to General Electric, but these latter organizations have yet to report any information. Some GaIn work for low rpm, space telescope slip ring application was reported by General Electric³ (Philadelphia), but was found to be inapplicable to the ARPA effort. Doctoral thesis work⁴ by Dr. Chabrier of Paris was also found to render little contribution to this effort. Current GaIn technology efforts of the General Electric Company, Ltd., of the U.K. are described in this writing.⁵ The liquid metal support systems task of this subject ARPA contract appears to be the most detailed, quantitative, engineering effort of its type in the rotating electro-mechanical machinery field.

5.2 CURRENT PROGRESS

5.2.1 Materials Selection and Compatibility Studies

This task has been established to select and evaluate NaK compatible materials for SEGMAG. In addition, as part of this study, a decontamination method has been established and tested. All the objectives, originally set up as part of this task, are being met on schedule.

Candidate SEGMAG materials have been defined, and to date, more than 1000 hours of cumulative NaK exposure time has been logged on more than 120 individual samples of these materials. These include: (1) rotor banding materials, (2) rotor bar insulation, (3) laminate composites, (4) potting compounds, (5) silastic elastomers, (6) coatings and paints,

(7) seal materials, (8) cooling fluids, (9) braze alloys, and (10) structural metals. The evaluation of candidate materials is proceeding through a defined test plan which was designed to incorporate the same material exposure sequence that will be followed during actual machine startup, decontamination, and requalification of components after decontamination and subsequent reassembly. Proposed materials are being exposed to commercial grade NaK in test canisters heated isothermally in a constant temperature oil bath. Figure 5-1 illustrates the glove box facilities which are being utilized to prepare and handle candidate materials and charge test canisters containing samples with NaK. Figure 5-2 is a view of the oil bath facilities in which the materials are thermally aged in a NaK environment.

All compatibility studies are being performed at 140°C for defined time intervals. This temperature was selected because, in all instances, it will be the most severe condition that any one machine component will see (machine hot spot temperatures were calculated to be 130°C max.). Therefore, it is assumed that materials which survive this condition in liquid NaK will be the prime candidates for the SEGMAG machine. In addition, materials are being evaluated at NaK exposure intervals of 100, 500, and 1000 hours by defined physical measurement techniques. Water has been employed as the NaK decontamination fluid. The antechamber of the glove box used for sample preparation is serving as a sample baking chamber, simulating machine pre-startup conditions of roughing pump vacuum at 100°C for a fixed time interval of 24 hours.

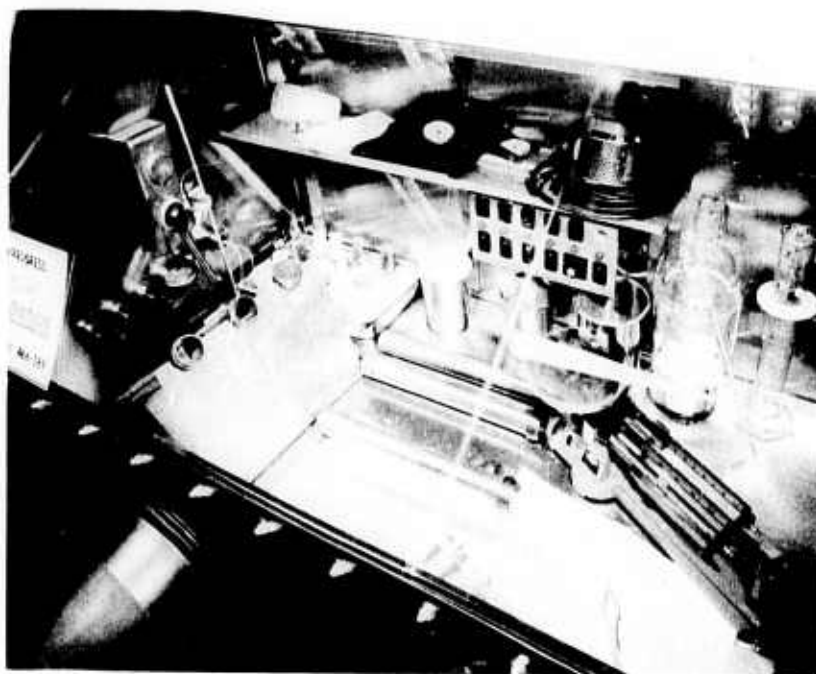
Physical testing for the materials evaluation includes: (1) weight changes, (2) dimensional changes, (3) hardness, (4) electrical resistivity, (5) flexural properties, (6) tensile properties, (7) mass spectrometry, (8) infrared spectroscopy, and (9) scanning electron microscopy.

Figure 5-3 illustrates the flow sequence that selected materials follow during NaK compatibility studies. This program is providing quantitative information (rather than just qualitative information) on the compatibility of materials with NaK. A number of materials have been defined for use in the SEGMAG demonstration machine and examples of both NaK compatible and incompatible materials are given below.

(1) Rotor Banding Material. An epoxy Novalac/glass fiber was selected as the rotor banding material. Since this material will serve as both electrical insulation and a NaK barrier to the rotor bar system, it is very important that its NaK compatibility be established. Selected material specimens were exposed to NaK and the compatibility was then established by tensile testing and scanning electron microscope examination. Table 5-1 lists the tensile test data for this material. Since the ultimate strength shows little change after more than 500 hours of NaK exposure, and since SEM examination shows that no material degradation has occurred, see Figure 5-4, this banding material is a prime candidate for use in the SEGMAG machine. Additional specimens will be tested after 1000 and 1500 hour NaK exposure time.

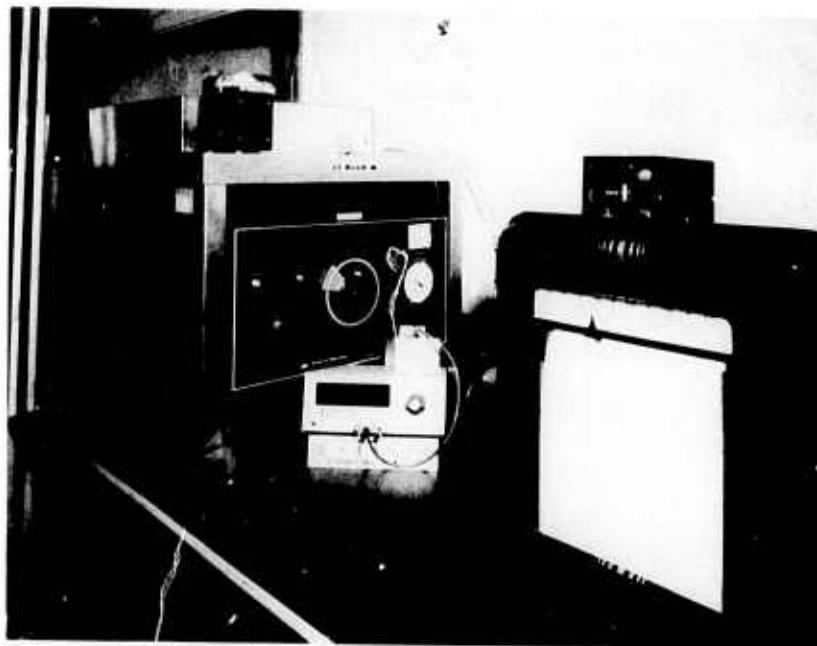


(a) General View of Facilities



(b) Samples of Materials Being Prepared
for NaK Compatibility Studies

Fig. 5-1—Glove box facilities utilized for the preparation and handling of materials being evaluated for NaK compatibility



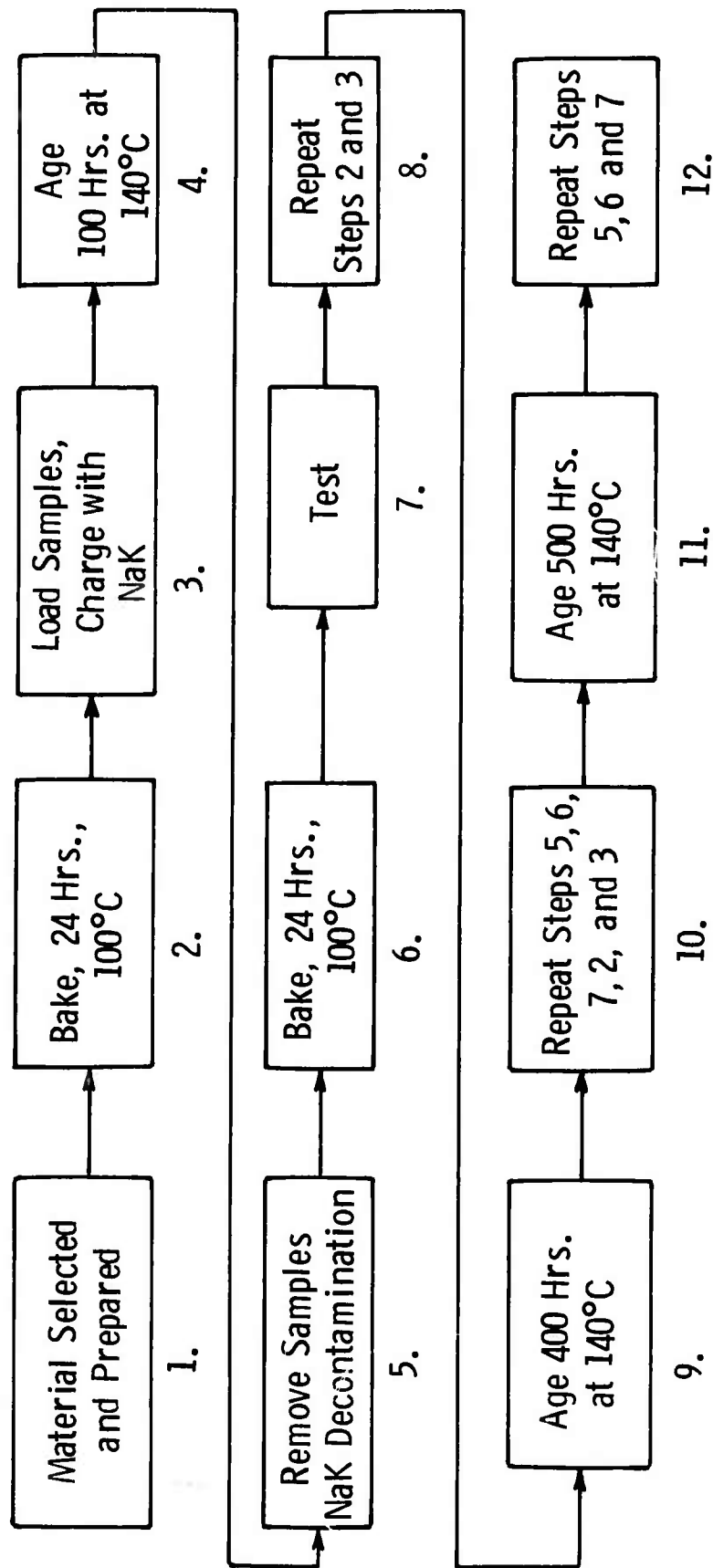
(a) View of oil bath, temperature monitor and recorder

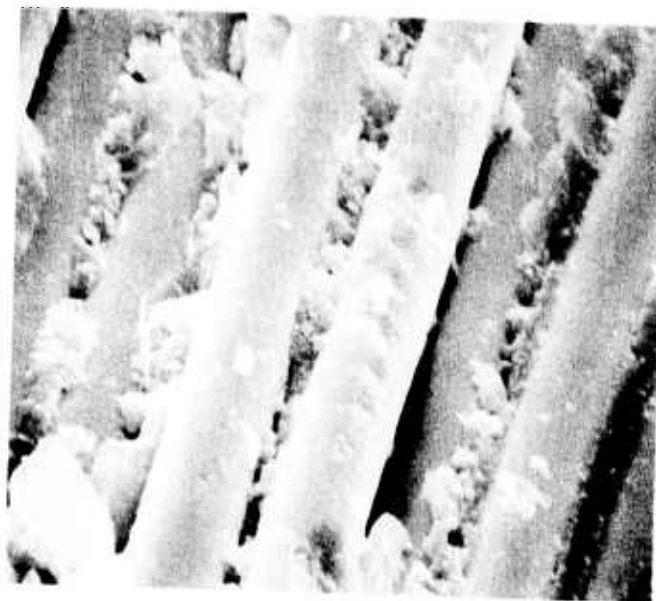


(b) View of material test canisters in oil bath

Fig. 5-2—Constant temperature oil bath facilities for the isothermal ageing of materials in a NaK environment

FIG. 5-3—SIMPLIFIED FLOW CHART OF MATERIALS COMPATIBILITY TEST PLAN





(a) Before NaK Exposure

30 μm



(b) After NaK Exposure

Fig. 5-4—Rotor banding material 431-S-2 (epoxy novalac resin/glass fibers) before and after NaK exposure at 140°C for 507.5 hours

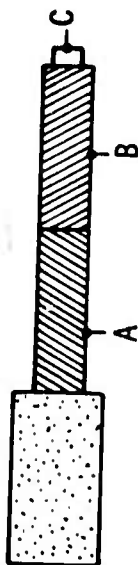
TABLE 5-1
 ROTOR BANDING MATERIAL 431-S-2
 (Epoxy Novalac Resin/Glass Fibers)
 Tensile Test Data

<u>Specimen I.D.</u>	<u>Specimen No.</u>	<u>Ultimate Strength (KSI)</u>
Archives	1	122.9
No NaK exposure	2	116.9
	3	131.0
	4	113.3
	5	121.0
	6	121.0
NaK exposed	7	142.8
99.5 hr	9	139.3
NaK exposed	8	132.2
507.5 hr	10	145.2

(2) Electrical and/or Rotor Bar Insulation. Electrical insulation systems detailed in the previous semiannual report have been evaluated for NaK compatibility.² Since no reported literature values could be found for NaK compatibility of materials of this type, insulation packages were defined from the NaK chemistry of organic systems. The general classification of selected insulation materials is listed below:

Conductor insulation	Kapton tape, glass supported acrylic tape
Ground wall	Epoxy bonded mica tapes
Outer binder tape	Epoxy, acrylic or highly modified polyester tapes baked with glass and/or organic fabrics

Test specimens were prepared and exposed to NaK at 140°C. Surface and volume resistivity measurements for insulation systems have shown that the selected materials qualify as NaK compatible (see Figure 5-5). Since these specimens were also decontaminated prior to electrical measurements, they also qualify as being compatible with the machine decontamination scheme. These results indicate that when little or no information is available on NaK compatibility, basic alkali metal chemistry can provide reliable guidelines in the selection of candidate materials.



Insulation System	Electrodes	Archives	Resistivity, Megohms		
			Heat, 112 Hrs.	Heat, 449 Hrs.	NaK, 449 Hrs.
1. Kapton Film 1/2 Lapped, Mica Bonded to Kapton Tape, Polyester on Dacron	A-C (Vol)	∞	∞	∞	∞
	B-C (Vol)	-	-	-	∞
	A-B (Surface)	∞	5×10^5	5×10^5	5×10^5
2. Kapton Film 1/2 Lapped, Mica Bonded to Kapton Tape, Epoxy on Dacron and Glass	A-C (Vol)	∞	10×10^5	∞	∞
	B-C (Vol)	-	-	-	∞
	A-B (Surface)	∞	∞	∞	10×10^5
3. Kapton Film 1/2 Lapped, Mica Bonded to Glass Tape, Polyester on Dacron	A-C (Vol)	∞	10×10^5	∞	37×10^3
	B-C (Vol)	-	-	-	∞
	A-B (Surface)	∞	∞	∞	∞
4. Kapton Film 1/2 Lapped, Mica Bonded to Glass Tape, Epoxy on Dacron and Glass	A-C (Vol)	∞	∞	∞	∞
	B-C (Vol)	-	-	-	∞
	A-B (Surface)	∞	10×10^5	10×10^5	∞

Note: $\infty > 10^6$ Megohms
Ageing Temperature = 140°C

Fig. 5-5—Resistivity measurements obtained on heat aged and NaK exposed electrical insulation systems

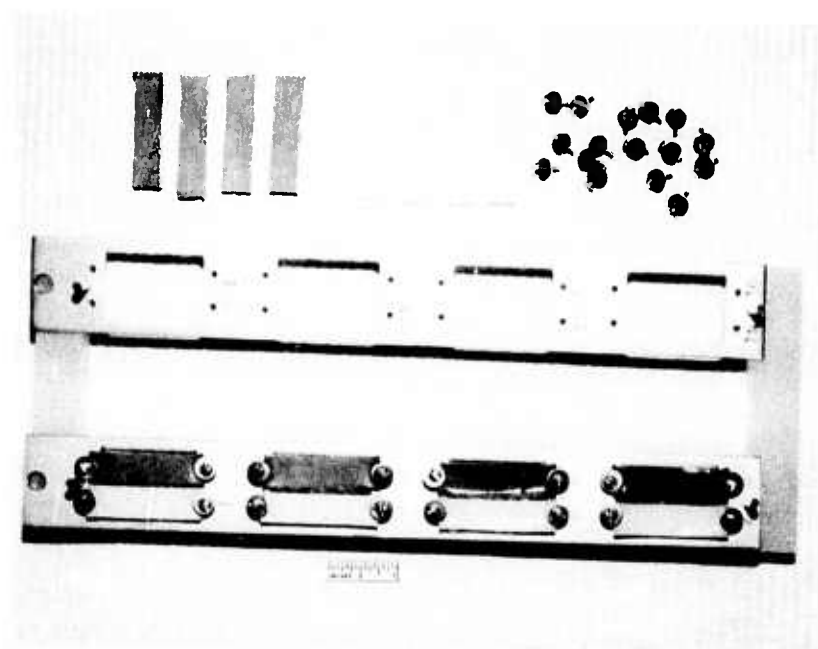
(3) Silastic Elastomers. During Phase I of this study, silastic elastomers were selected as probable sealing materials for use in the SEGMAG demonstration machine.¹ Compatibility studies have shown that although these materials are compatible with NaK at room temperature ($\sim 25^{\circ}\text{C}$), severe degradation occurs at elevated temperatures (140°C). Figure 5-6 illustrates the type of failure demonstrated by silastic elastomers exposed in a NaK environment at 140°C for 100 hours. As a result of this study, silastic elastomers have been found to be incompatible with the NaK environment and will not be utilized in the SEGMAG machine.

(4) Machine Laminates. A number of laminate composite materials are currently being evaluated for NaK compatibility. In addition to noting weight and dimensional changes, flexural properties are also being determined. From these measurements, trends are being established for the ultimate stress and elastic modulus of these materials as a result of NaK exposure. Examples of the type of plots being obtained are shown in Figure 5-7. With this type of quantitative information, extrapolation to extended material lifetimes may be determined. Additional data for longer exposure time (>1000 hours) are currently being obtained.

(5) Braze Alloys. It has been known for some time that microbraze alloys are compatible with NaK. On the other hand, soft solders of tin/lead compositions are incompatible even for very short periods of time. Silver solders may be employed, but very little quantitative information is available concerning the compatibility of these braze alloys with NaK. This study has attempted to determine whether or not selected silver braze alloys may be employed in the SEGMAG demonstration machine. Since all the braze joints will be protected from the NaK environment by the rotor banding material, total braze alloy compatibility is not essential. However, in the event that NaK breaches the protective barrier of the rotor banding material, the most compatible alloy must be selected. A total of five silver braze alloys have been evaluated for NaK compatibility at 140°C to a maximum exposure time in excess of 500 hours. Table 5-2 presents a tabulation of the various alloys studied and the weight changes which were observed at exposure times of 112 and 593 hours.

TABLE 5-2
BRAZE ALLOYS EVALUATED FOR NaK COMPATIBILITY AT 140°C

Sample I.D.	Composition	% Weight Change		Visual Observation
		112 hr	500 hr	
BAG-8	72% Ag, 28% Cu	-1.5	-4.03	OK
BAG-18	60% Ag, 30% Cu, 10% Sn	-0.6	-0.44	OK
BT-Li	71.8% Ag, 28% Cu, 0.2% Li	-0.4	-0.69	OK
BCuP-5	15% Ag, 80% Cu, 5% P	+2.1	-4.25	Severe attack, Failed
BAu-4	81% Au, 18.5% Ni	-71.0	--	Sample dissolved



(a) Silastics as Prepared - Before NaK Exposure



(b) Silastics After NaK Exposure

Fig. 5-6—Silastic elastomers (116 RTV and RTV 732) before and after NaK exposure at 140°C for 100 hours

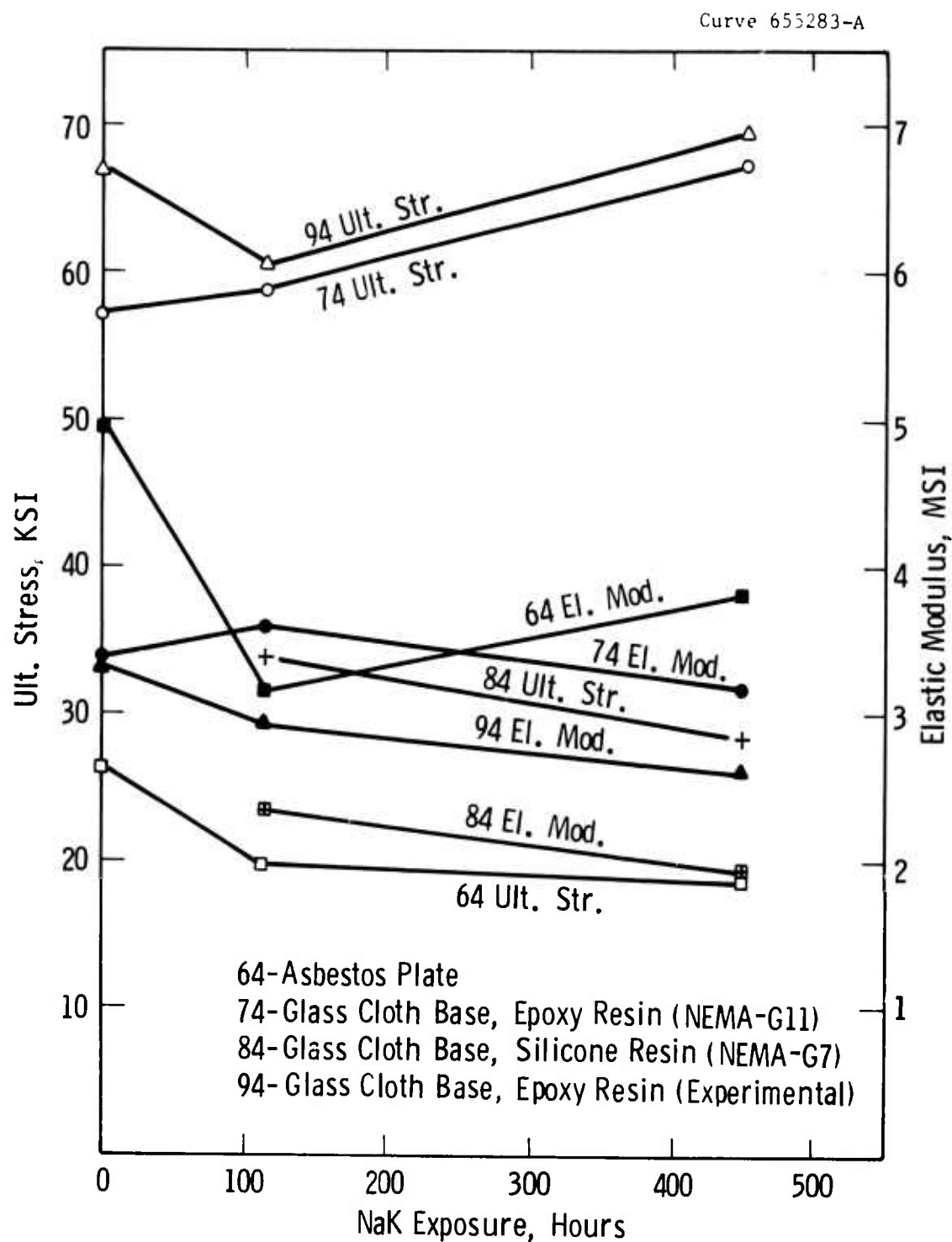


Fig. 5-7— The change in ultimate stress and elastic modulus of candidate laminate materials as a result of NaK exposure at 140°C

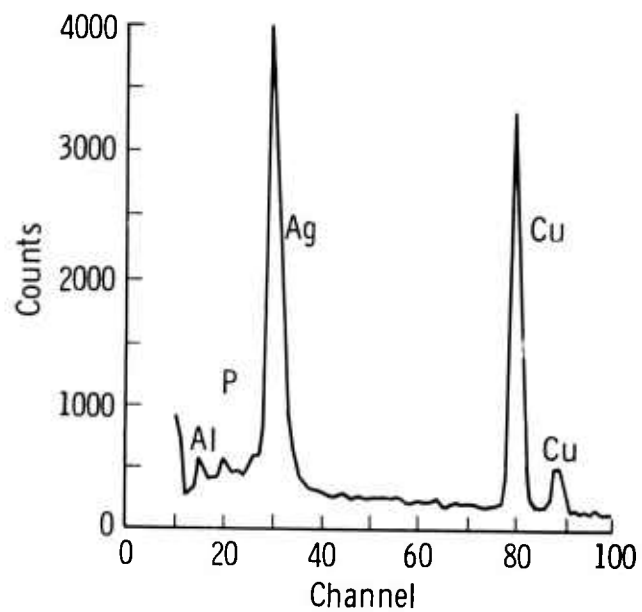
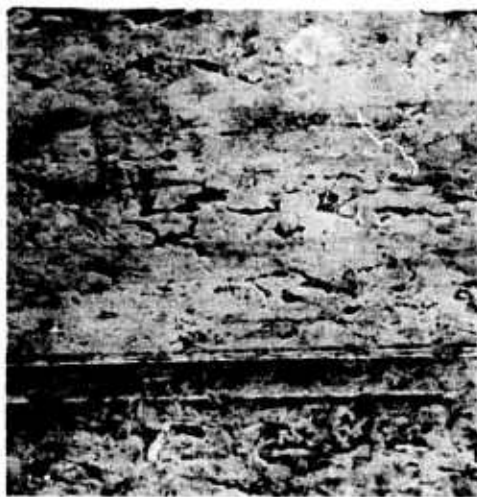
Note that two (BCuP-5 and BAu-4) of the five braze alloys completely failed in 112 hours. SEM studies carried out on these materials have indicated that the failure mechanism occurs by the selective leaching of precious metals (silver or gold) from the alloy matrix. Figures 5-8 and 5-9 show SEM micrographs of the severely attacked braze alloys before (a) and after (b) exposure. Also shown is the backscattered X-ray spectrum which defines the composition of the alloys before and after NaK exposure. Note that in each instance the precious metal has been depleted in the NaK-exposed material when compared with the as-received material. The three remaining materials have also lost weight via the removal of silver from the alloy matrix, but these small losses occur only under the most severe NaK exposure conditions. Because of the protective barrier defined by the rotor banding material, it is not anticipated that NaK will reach the braze joints. If this does occur, the selected braze alloys should tolerate the environment until repairs can be made.

5.2.2 Liquid Metal Loop and Cover Gas Systems

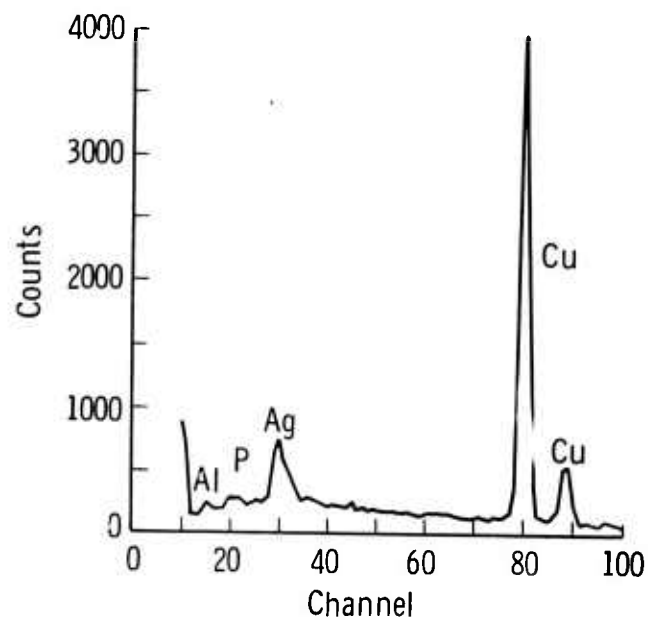
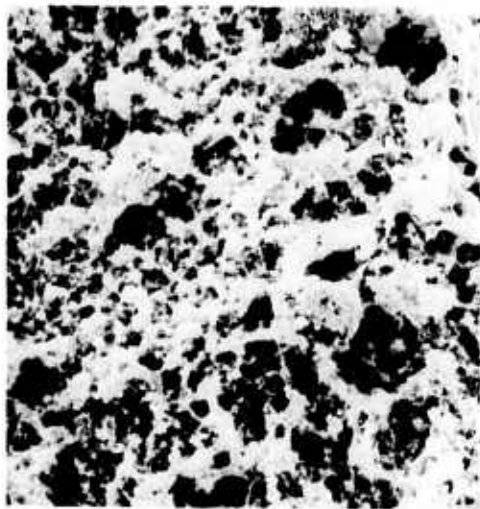
The NaK recirculation and purification loops for the SEGMAG demonstration machine have several performance criteria to meet. These criteria have been made demanding for the prototype machine to allow operational flexibility and the evaluation of machine-loop interactions. The NaK loops have been required to perform at flow rates of 0 to 800 cc/min at pressures of 0 to 10 psig, at temperatures of 0 to 180°C, at cover gas impurity levels (O_2 , $H_2O(v)$) of 0 to 100 ppm. The loops can operate under batch, continuous, or intermittent NaK recirculation, and under machine vibrations. They have had to demonstrate extended life capability, and to maintain operational fluid levels and purities in the current collector zone of the machine.

Original design plans considered one large NaK loop with six parallel feed-drain legs for current collection fluid circulation.² Problems were apparent when the I^2R losses were considered for common NaK current collection lines. Losses of over 40 kW were predicted. A technique of breaking the NaK flow into slugs and utilizing one NaK loop demonstrated that electrical isolation of the current collectors could be maintained. However, verification of this novel NaK recirculation technique for extended, unmanned operation was considered too time consuming to contract schedules, and a more secure approach was followed.

A small NaK loop was designed to service each separate current collector of the SEGMAG. Each loop was thus an electrically isolated, individually controllable NaK supply system. Figure 5-10 presents the schematic of such a loop. In this design, NaK drains from the current collector sump region with the assist of a gas pump for cover gas removal, into a large sump tank. The sump tank is capable of holding the entire loop NaK inventory, and thus cannot overflow into the gas pump system. Also,



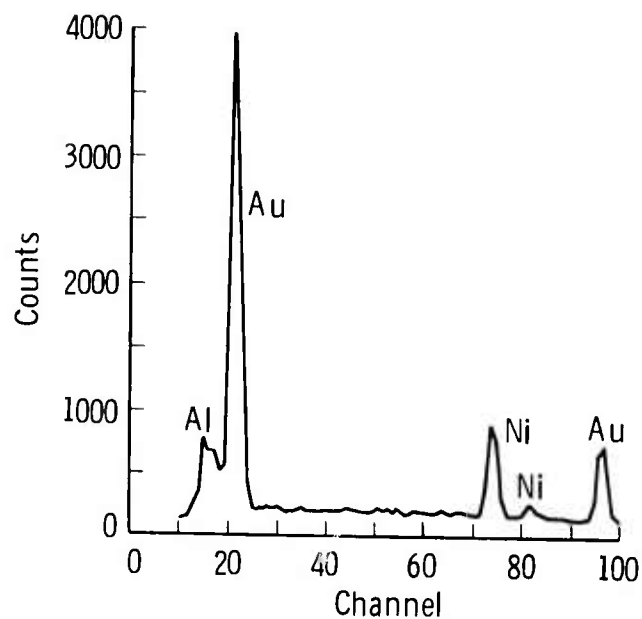
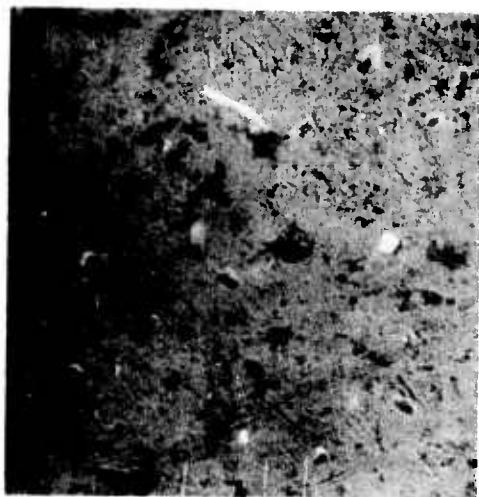
(a) Before NaK Exposure



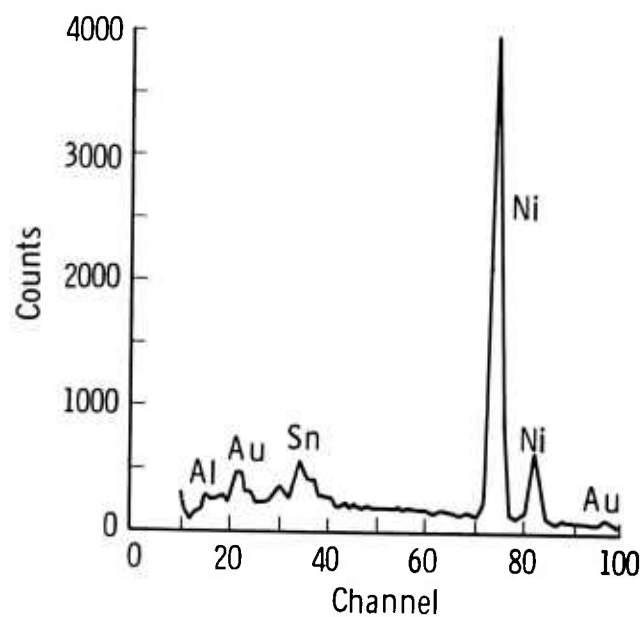
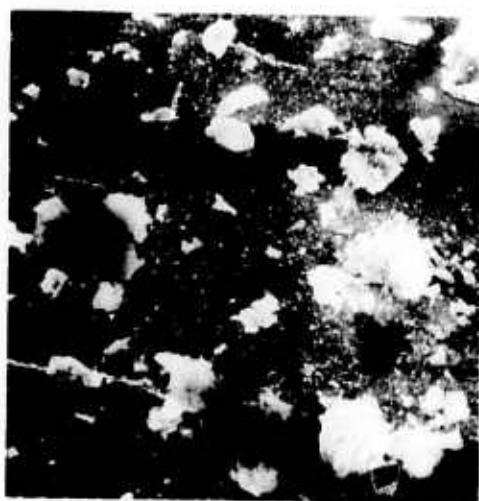
(b) After NaK Exposure

← 25 μ m →

Fig. 5-8— Braze alloy BCuP-5 (15% Ag, 80% Cu, 5% P) before and after Nak exposure at 140°C for 112 hours



(a) Before NaK Exposure



(b) After NaK Exposure

← 25 μ m →

Fig. 5-9— Braze alloy BAu-4 (81.5% Au, 18.5% Ni) before and after NaK exposure at 140°C for 112 hours

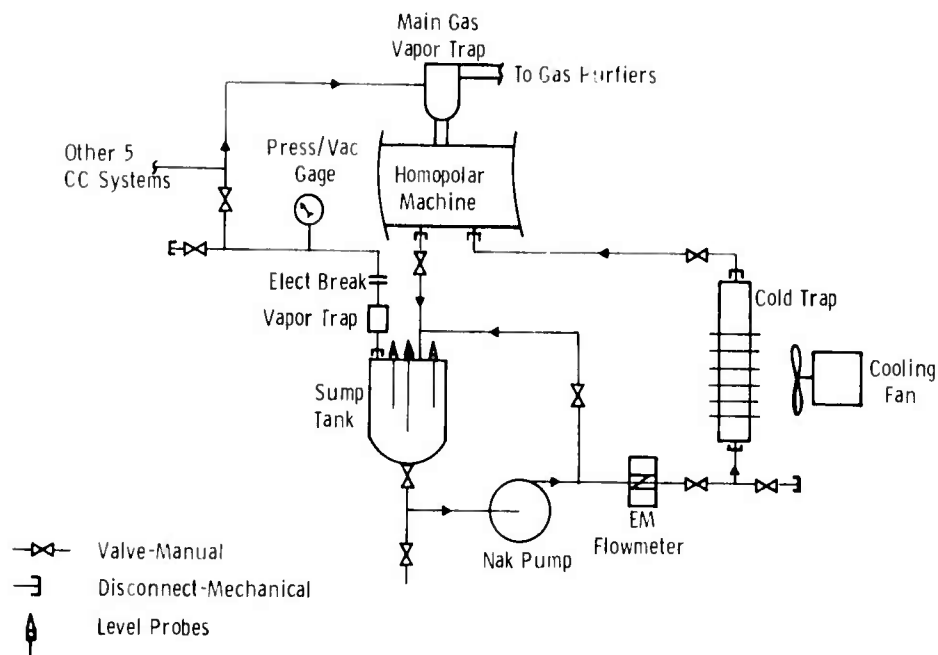


Fig. 5-10—Small NaK loop concept for servicing each current collector independently

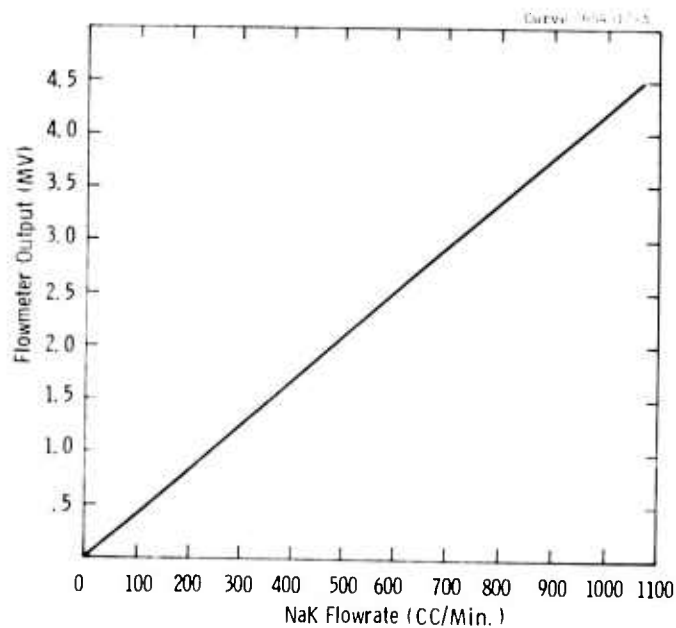


Fig. 5-11—Calibration of NaK flowmeter for 35.6 cm current collector test stand (19-19-73). Flowmeter temperature = 42°C

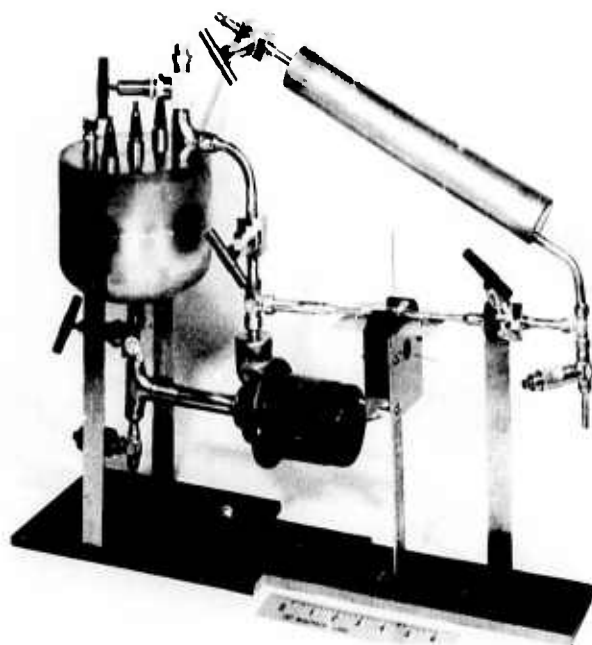


Fig. 5-12—Assembled NaK loop for current collector service in prototype SEGMAG machine

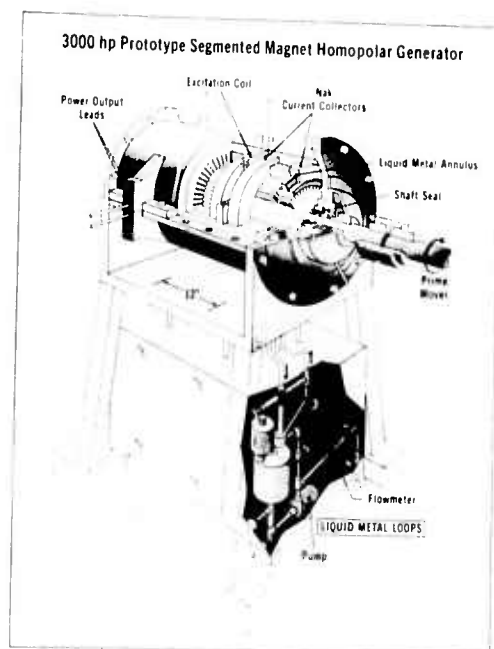


Fig. 5-13—Illustrating placement of six current collection NaK loops beneath SEGMAG machine

level probes indicate whether NaK levels are becoming unacceptably high or low. The sump tank provides the first stage of NaK purification in that insoluble or precipitating oxides and impurities will float to the surface of the NaK.

The NaK pump was selected after evaluating EM, gear, bellows, and centrifugal pumps. It is a canned motor, inductively coupled, centrifugal pump and was qualified for over 1000 hours in NaK prior to its selection. The flowmeter is electromagnetic, and was designed by Westinghouse for low temperature-low flowrate NaK service. A calibration curve presented in Figure 5-11 demonstrates the meter's accuracy to ± 5 cc/min in the 0-800 cc/min range.

In the loop, the NaK flows from the flowmeter up through a cold trap, which removes soluble impurities and oxides by a precipitation process and particulates by a filtering process, before returning NaK to the current collector. Figure 5-12 presents one of the SEGMAG NaK loops. Components can be identified from Figure 5-10. The loops are of type 304 stainless steel, and consist of all welded, inspected construction, employing liquid metal bellows seal valves. Loop capabilities are presented in Table 5-3. As presented in Table 5-3 and demonstrated in Figure 5-13, the six NaK loops will be placed beneath the SEGMAG unit.

A prototype SEGMAG loop was charged with NaK and installed for endurance and acceptance testing. The NaK was pumped over a 4-foot rise into a glass vessel which was exposed (open) inside a glove box with nitrogen cover gas. NaK recirculation was maintained at 200 cc/min for 500 hours without signs of degradation in loop performance. For the next 500 hours, the glove box atmosphere was bubbled through the NaK in the glass vessel at 700 cc/min, again without degradation of loop performance, or loss of metallic luster at the exposed NaK surface. A beaker of stagnant NaK placed beside the recirculation vessel developed a thick black oxide coating during this 1000 hour test cycle.

The outgassing and volatile gas species of typical machine organic insulating materials were analyzed by gas mass spectrographic techniques, and a special cylinder of gas containing the mixture of gases found in the proper ratios was obtained from a vendor. The second 1000 hours of loop testing will include the bubbling of this prototype machine gas composition through the glass vessel containing the endurance test loop to evaluate the loop's capability to purify NaK exposed to this atmosphere.

Table 5-4 reviews the parameters of the NaK loop endurance test. As also noted in Table 5-4, the prototype NaK loop servicing the 35.6 cm current collector test stand has incurred severe operating conditions of variable flow rates from 0 to 800 cc/min, cover gas impurity levels up to 80-100 ppm oxygen, moisture, carbon dioxide, and at one time, inadvertent exposure to air being pumped through the sump tank by a gas pump. This NaK loop is still operating as a viable, on-line functional test of loop design and capability.

TABLE 5-3

NaK Loop Capabilities

- | | |
|--------------------|--|
| 1. Temperature: | Max. 250°C loop, 150°C pump
Min. 0°C loop and pump |
| 2. Flowrate: | 0-800 cc/min |
| 3. Inventory: | Sump tank volume - 2700 cc
NaK charge in system - 2000 cc
Total working NaK - 850 cc |
| 4. Physical size: | Each loop 2' x 2' x 7' wide
Six loops fit into 2' x 2' x 3' long |
| 5. Pressure: | Max. 50 psig loop, 15 psig pump
Min. high vacuum loop, 0 psig pump |
| 6. Material: | All 304 s/s or 316 s/s
Valves - Metal bellows seal welded
All welded, inspected construction |
| 7. Purity control: | Two stages
First stage - Sump tank, oxides float
Second stage - Cold trap, filter |
| 8. Level control: | Sump tank - Three electrical
continuity probes |

Dwg. 6220A / /

TABLE 5-4

NaK LOOP ENDURANCE TEST

Purpose: To qualify the NaK loop as a system for extended term operation under prototype machine cover gas environments.

Current Status:

- Over 500 hours (11-30-73) operation
- Continuous flow rate at 200 cc/min
- Flowing into open vessel exposed to cover gas/contaminant mixture
- Operating unattended
- Sump tank level probes operational
- Operating without problems

Additional qualification data:

Similar NaK loop operated for over 200 hours on 14-inch current collector test stand. Operating conditions in terms of temperature, duty cycle, impurity exposure, etc. much more severe than expected commercial field exposure.

The protective, inert cover gas recirculation and purification system for the SEGMA²G demonstration machine was designed to satisfy several diverse criteria. The goals of the cover gas system include: (1) maintenance of liquid metal purity by removing outgassed and in-leaking impurities; (2) conservation of gas by recirculating gas for purification, thus restricting gas makeup for losses; and (3) diminishing the size of the gas inventory which must be maintained for machine operation.

A versatile cover gas recirculation and purification unit was designed and constructed. The basic system consists of a blower and tandem purification towers (regeneratable) for the removal of oxygen and moisture. Refrigerant cooled inlet and exhaust lines prevent the circulation of NaK vapors and volatile hydrocarbons. Figure 5-14 illustrates the conceptual gas system while Table 5-5 describes the cover gas system operating capabilities. Figure 5-15 presents the basic gas purifier station of Figure 5-14, and shows the blower, tandem purification towers, automatic switching valves, etc. The station is still undergoing qualification testing on a large glove box into which basic NaK contaminating gas impurities (i.e., oxygen, moisture) are being introduced. Performance has been acceptable.

An analytical model projecting NaK contamination levels (as Na₂O) as a function of: (1) NaK recirculation rate and thus dwell or reaction time inside the machine; (2) cover gas recirculation rate; and (3) cover gas impurity (ppm oxygen) level maintained inside the machine, has shown that batch operation of NaK in the current collectors is untenable. Saturation levels of Na₂O in NaK are quickly exceeded even under cover gas systems of very low oxygen content and minimal recirculation. The model is now being employed to determine an optimum cover gas recirculation rate matched to the outgas rate of volatile materials impurities.

The balance of the cover gas system has been finalized, and components have been ordered. Several critical components such as gas pumps, flowmeters, and pressure maintenance units have been performance tested prior to their design commitment to the cover gas system.

An instrumentation and control panel similar to that described in the last semi-annual report² for the 35.6 cm current collection test stand is under construction for the SEGMA²G machine. The instrumentation, readouts, and controls were qualified and accepted through their performance on the 14-inch current collector test stand.

An electrolytic GaIn purification cell was evaluated during an intensive performance test of the General Electric Company, Ltd., homopolar machine.⁵ The GaIn eutectic was continuously recirculated through the machine at flowrates up to 60 cc/min, under argon cover gas impurity levels of up to 3000 ppm moisture, 100 ppm nitrogen, and 15 ppm oxygen. (Levels above 15 ppm were not observed because most oxygen was believed to have reacted with the GaIn.) The GaIn flow system consisted of Teflon

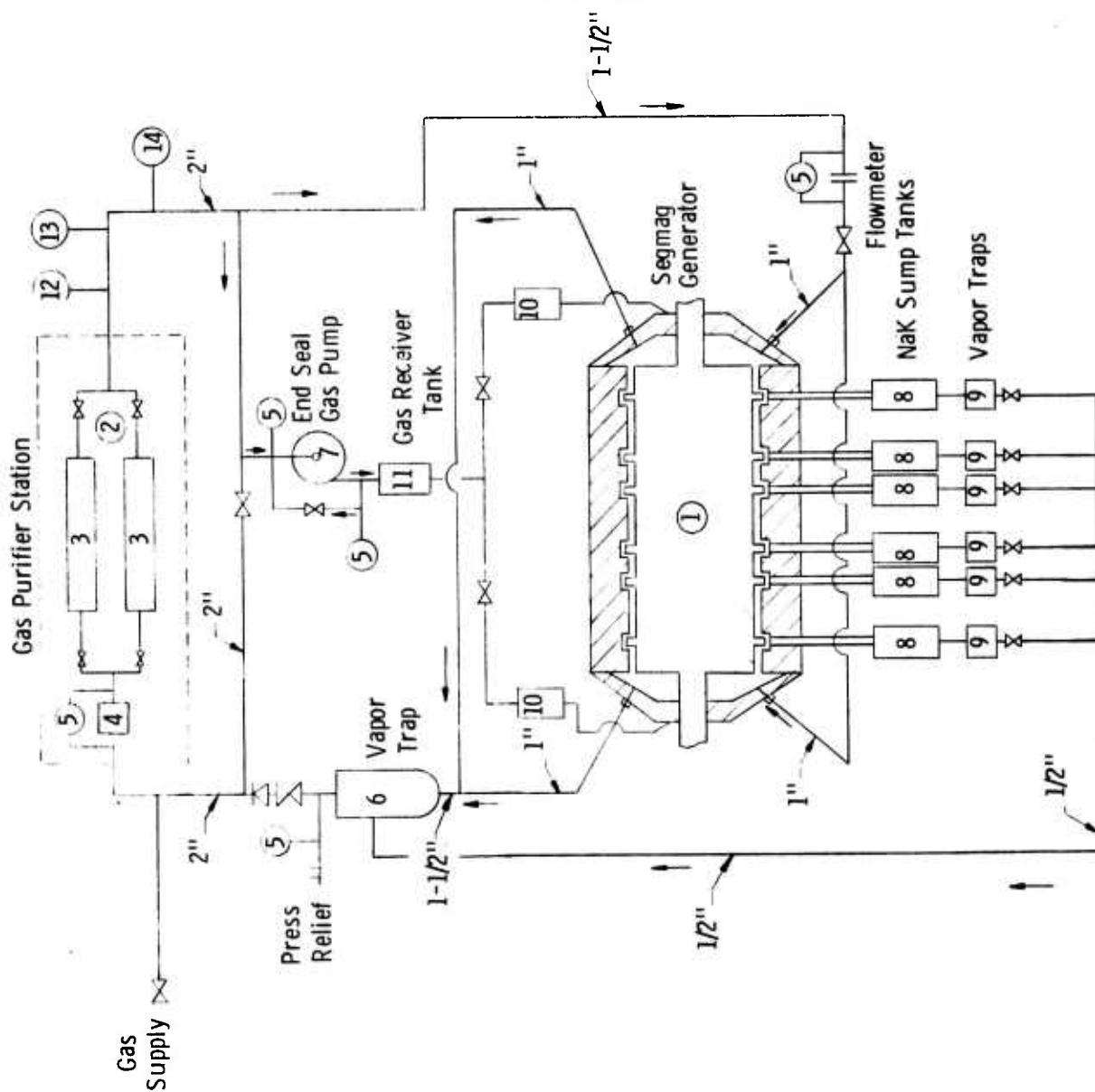


Fig. 5-14 - Prototype segmag generator cover gas system

1. Prototype Segmag Generator
2. Gas Purifier Station with Automatic Pressure Control and Automatic Regenerator Sequence
3. Compound Purifier Towers
4. Gas Pump - 40 CFM @ 30" H₂O
5. Pressure Gage
6. Vapor Trap (Special)
7. Gas Pump - 1.7 CFM @ 10 psi ΔP
8. NaK Sump Tank
9. Vapor Trap
10. Flowmeter (Gas)
11. Receiver Tank (Gas)
12. Moisture Analyzer
13. Oxygen Analyzer
14. Combustible Gas Detector

TABLE 5-5

COVER GAS SYSTEM CAPABILITIES

Gas:	Nitrogen
Recirculation Rate:	Up to 35 CFM
Purity Maintenance:	1 ppm Oxygen 2 ppm Moisture Experimentally Verified
Operating Pressure:	Machine housing at 35" H ₂ O positive pressure gradient
Heat Exchanger:	Has freon cooled inlet and outlet lines
Operation:	Continuous On-Line. One tower on-line while other is regenerating. Regeneration sequence is automatic
Make-up Gas:	Automatically supplied when required
Monitors:	Delphi Oxygen Analyzer (ppm range) Westinghouse Oxygen Analyzer (ppm range) Panametrics Moisture Monitor (ppm range) Machine Pressure (regulated) Gas Flow Rate Regeneration Cycle Timer
Shaft Seals:	Supplies cover gas at 5 psi ΔP to shaft seals via a gas pump



Fig. 5-15—Internal components of central gas purifier station for the SEGMAG homopolar machine

tubing and a Teflon diaphragm in the pump. Fluid drainage from the machine was assisted by centrifugal force. Observable black oxides were removed from the effluent GaIn in a clear, plastic, electrolytic reclamation cell. Reclamation occurred beneath a layer of sodium hydroxide and continued as an on-line process. Extensive GaIn loop, purification, and compatibility tests are planned.

5.3 REFERENCES

1. "Design and Development of a Segmented Magnet Homopolar Torque Converter," ARPA Contract DAHC-15-72-C-0229, Semi-Annual Technical Report for Period Ending November 30, 1972, (Ⓜ Report No. EM 4471), December, 1972.
2. "Design and Development of a Segmented Magnet Homopolar Torque Converter," ARPA Contract DAHC-15-72-C-0229, Semi-Annual Technical Report for Period Ending May 31, 1973, (Westinghouse Report Number EM-4518), June, 1973.
3. S. M. Weinberger, "Development of a Liquid Metal Slip Ring," NASA-CR-120885, November, 1972.
4. J. P. Chabrezie, Ph.D. Thesis, University of Paris, March, 1973.
5. F. G. Arcella and D. C. Litz, "Performance Test of the GEC 36G-II Homopolar Generator," Trip Report Number PIC-74-1, December, 1973.

SECTION 6

SEAL STUDY

6.0 OBJECTIVES

The primary goal of this task is to develop a shaft seal to avoid contamination of the SEGMAG machine's containment vessel by either air, moisture, or the hydrocarbon-based fluid used for bearing lubrication and thereby prevent contamination of the liquid metal system. In addition, excessive losses of the machine's inert cover gas to the atmosphere must be avoided.

The specific objectives of this task during the Phase II portion of this program are as follows:

- Construct a seal test stand capable of evaluating the performance of tandem circumferential seals in a dry, inert environment.
- Perform functional seal tests at 3600 rpm in dry nitrogen gas on seal units equipped with composite-type seal materials capable of retaining their self-lubricating ability in a no-moisture environment.
- Perform functional endurance tests on that combination of seal design and material which demonstrate optimum performance with respect to gas leakage, seal wear, operating temperature, and NaK compatibility.

Complementing this portion of the program are two supporting efforts designed (a) to evaluate the compatibility of a variety of candidate seal materials with NaK (reported in 5.2.1), and (b) to determine the friction-wear characteristics of these seal materials in face seal screening tests.

6.1 PRIOR AND RELATED WORK

Studies performed during the Phase I effort of this program indicated that a tandem circumferential seal,^{1,2} or bore seal, was the prime candidate for satisfying the requirements imposed on the primary rotor shaft. The circumferential seal not only exhibits the ability to withstand high velocity rubbing at its primary sealing surfaces, but also the ability to provide a high degree of sealing effectiveness. Its design conserves weight and space, provides virtually unlimited shaft travel, and is easily assembled. The seal ring itself is enclosed by a cover ring to close off joint leakage. Joints on the seal and cover ring segments are staggered to minimize leakage at these locations. The segments are usually held in place by Inconel X garter springs.

The runners against which the seal operates are made as replaceable shaft sleeves of hard chrome plate or Linde flame-sprayed tungsten carbide. The geometry of the runner is as important as that of the seal. It must be sealed to the shaft to prevent leakage past itself and the shaft. Runner faces must be truly flat and should be clamped to a shaft shoulder with no distortion. Figure 6-1 is a schematic of this seal type.

With regard to material selection for use in these seals, care must be exercised to insure that the self-lubricating composite employed retains its lubricating ability in a no-moisture, inert gas environment. In this respect, a recent Westinghouse supported program³ directed toward the evaluation of seal materials for liquid metal pump cover gas systems has shown that standard grades of carbon-graphite seal materials exhibit extremely poor friction-wear characteristics in dry argon.

Based on the decision to utilize the tandem circumferential seal as the rotor shaft seal, a seal test stand was designed during the Phase I effort of this program. Figure 6-2 is a schematic of the device and provides an overall view of the drive motor, support frame, and the seal test stand itself. Figure 6-3 is a more detailed view of the test stand, illustrating slave bearing preload techniques and test seal mounting and locking arrangement. The drive motor is a 10 hp, 3 phase, 230 volt adjustable speed drive with a static dc thyristor drive control. Maximum operating speed of the motor is 3600 rpm, regulated to within + 1% by means of a separate tachometer unit. The motor is equipped with jogging and reversing capabilities as well as dynamic braking. Through the use of a 2:1 pulley ratio, the test stand is capable of performing experiments on various seal configurations over a 7000 rpm speed range in inert, bone-dry environments. Leakage rates, operating speed, and seal and bearing temperatures are continuously monitored. The test stand is capable of evaluating seals for shafts ranging in diameters from 2 to 6 inches. Figure 6-4 is a photograph of this test rig.

6.2 CURRENT PROGRESS

The test program for functional seal testing consists of three phases:

- 1) Candidate seal materials are being evaluated with regard to their ability to operate effectively in an inert, no-moisture environment.
- 2) Concurrently, these materials were evaluated with respect to their compatibility with NaK at room temperature and, where appropriate, at elevated temperature.
- 3) Finally, the most promising materials are being fabricated into actual seals and tested extensively with respect to operating speed, runner design and material, and load pressure. The results will be compared against those obtained on units employing standard carbon-graphite materials. Parameters monitored during these tests will include seal wear, leakage, and operating temperature. Progress in these areas is described below.

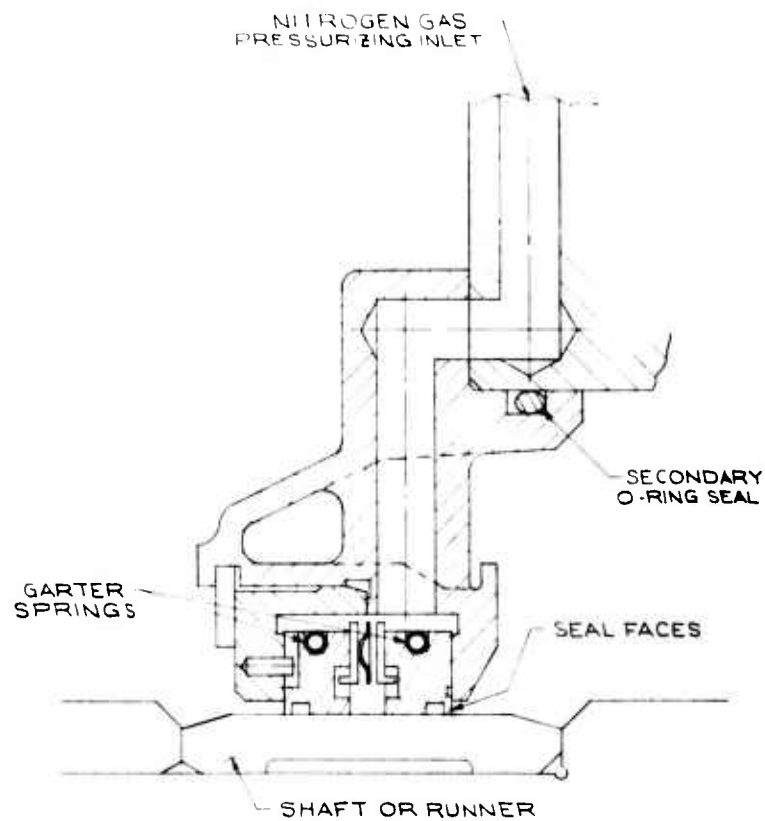


Fig. 6-1—Schematic of typical tandem circumferential seal

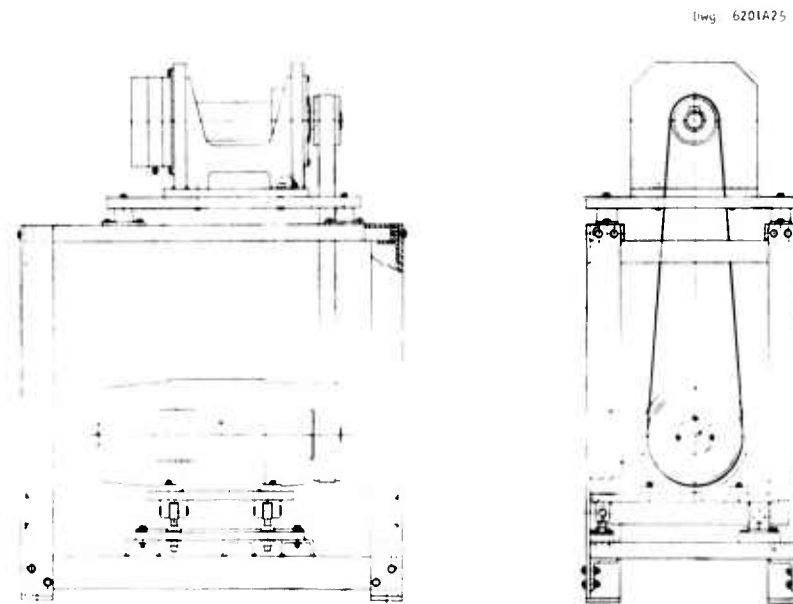


Fig. 6-2—Shaft/containment vessel seal test stand

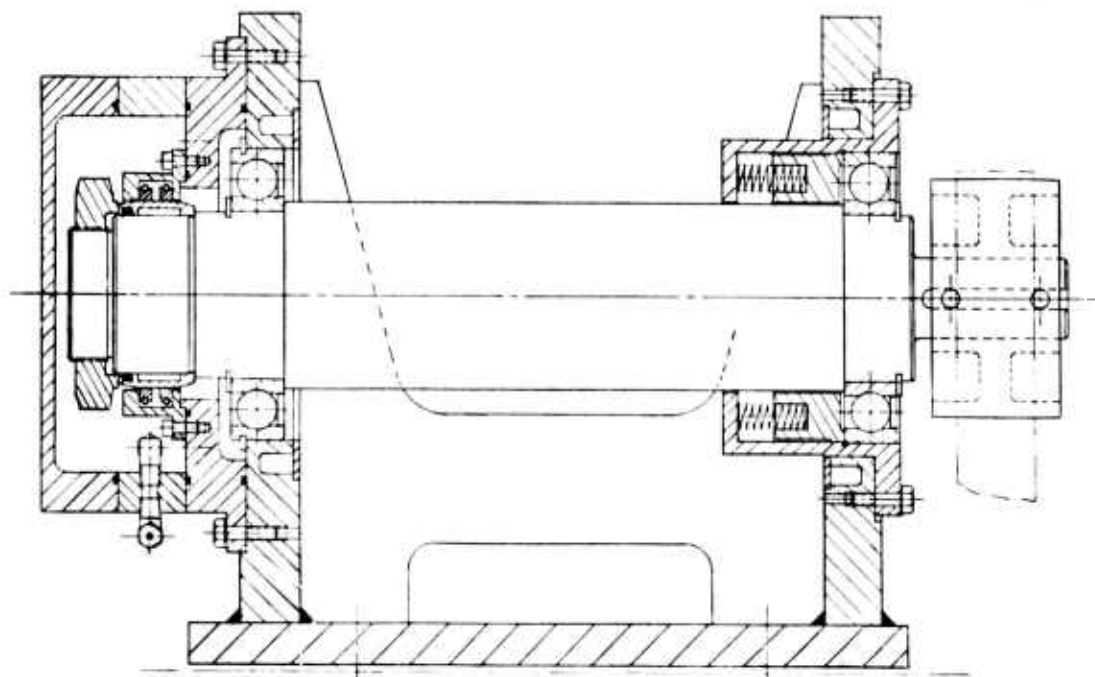


Fig. 6-3—Details of seal test device

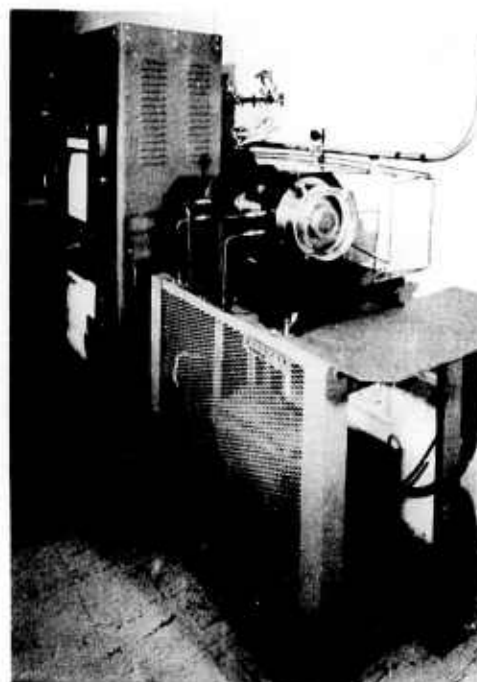


Fig. 6-4—Tandem circumferential seal test rig

6.2.1 Face Seal Screening Tests

As discussed in Section 5.2.1 of this report, preliminary NaK exposure studies on conventional and filled carbon-graphite seal materials quickly illustrated their total lack of compatibility with the liquid metal. As a result, the number of candidate seal materials suitable for this application was severely limited. Table 6-1 lists those materials selected on the basis of (a) their potential compatibility with NaK, and (b) their ability to retain acceptable self-lubricating characteristics in an inert, no-moisture environment.

TABLE 6-1
CANDIDATE SEAL MATERIALS FOR USE IN SEGMAG
PRIMARY ROTOR SHAFT SEALS

Material	Composition	Supplier
Delrin "AF"	Acetal matrix + PTFE fibers	Dupont
WGI	Tungsten Diselenide + Gallium-Indium	Westinghouse
Meldin P-30	Polyimide matrix + PTFE	Dixon
SP-3	Polyimide matrix + MoS ₂	Dupont
SP-211	Polyimide matrix + PTFE + Graphite	Dupont

Prior to fabricating these materials into actual circumferential seals, each composition was evaluated on a face seal test apparatus with respect to its dynamic friction coefficient, wear rate, and ability to retain self-lubricating characteristics in an inert, no-moisture environment. Figure 6-5 is a schematic of the test apparatus used to perform these tests. Operation of this unit at PV (pressure \times velocity) ratios up to 100,000 and temperatures up to 450°F is possible.

The candidate seal material is fabricated into a face seal having a 2-7/8" diameter sealing dam and is dead-weight loaded against a Kennametal WC801 tungsten carbide runner mounted in a KOVAR housing. The runner is driven at a constant speed of 3600 rpm. Through the use of a metal extension and glass bell cover, a sealed test chamber is provided in which the type of environment (air, nitrogen, helium, etc.) and its moisture content can be carefully controlled. Test parameters monitored during each experiment include the dynamic friction coefficient of the seal material with respect to the rotating runner, seal face wear, and operating temperature. Tests on the candidate materials were conducted at ambient temperature and a surface velocity of 41 fps in a nitrogen gas environment having a dew point < -45°C. It will be noted that high dynamic friction coefficients actually caused melting of the Delrin "AF" composite under a unit loading of 30 psi. Both the WGI and Meldin P-30 self-lubricating

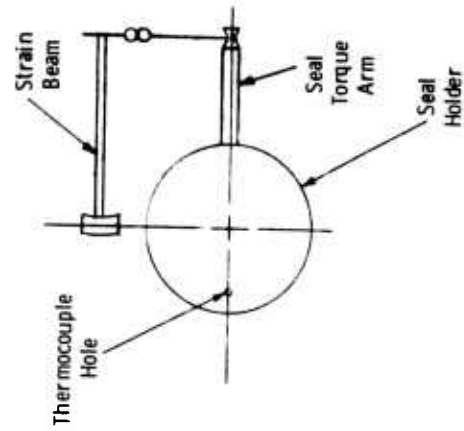
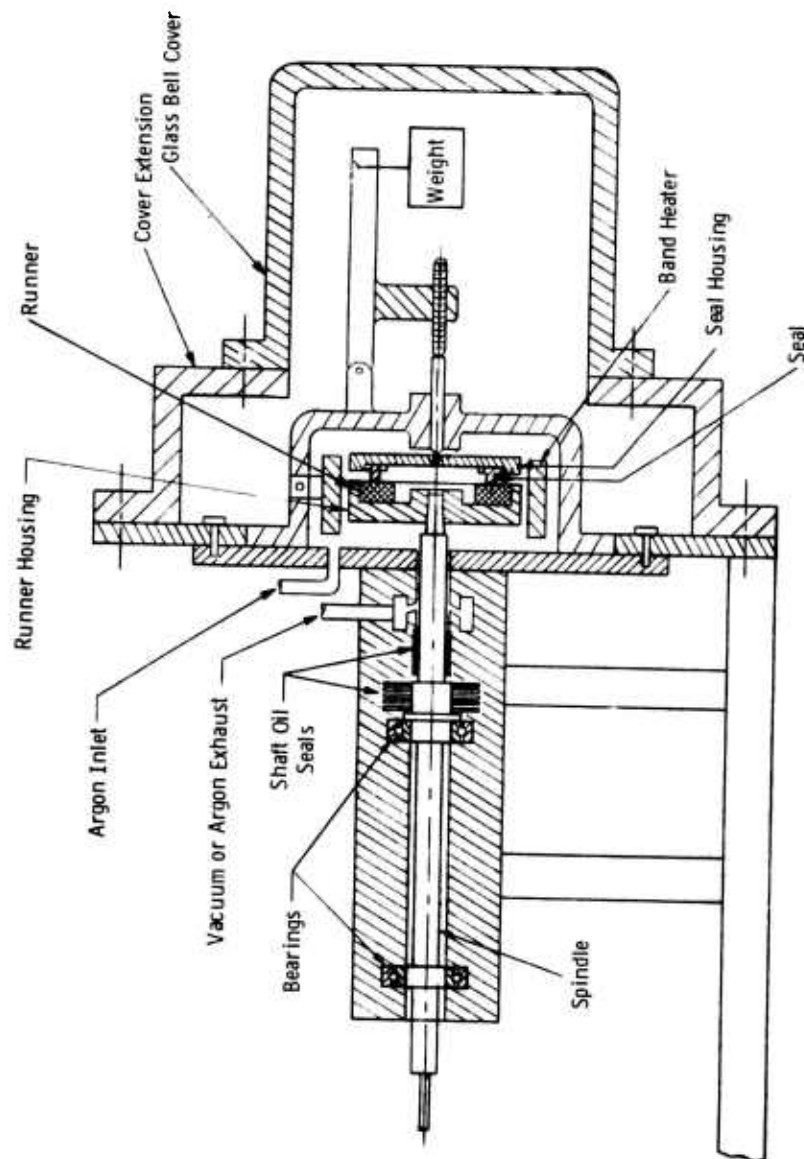


Fig. 6-5—Face seal screening test apparatus

composites demonstrated excellent friction and wear characteristics over continuous 140 and 200 hour runs, respectively. Unfortunately, later studies with regard to the compatibility of these materials with NaK eliminated them from further consideration at this time. It will be noted from data in Table 6-2 that both polyimide matrix materials (SP-3 and SP-211) exhibited quite high dynamic friction coefficients when operated under unit pressures of 15 psig. Upon reducing this loading to 2.6 psig, however, that material containing PTFE and graphite as fillers (SP-211) performed well with respect to both friction coefficient and wear rate. NaK compatibility studies complementing this seal material development effort (see Section 5) also indicated that the material was indeed compatible with the liquid metal at temperatures up to at least 108°C.

TABLE 6-2
FACE SEAL TEST RESULTS ON CANDIDATE SEAL MATERIALS

Seal Material	Face Load-psi	Time Hours	Wear Mils	Friction Coefficient
Delrin "AF"	30	High Friction Caused Melting		
WGI	15	140	0.4	0.03
WGI	30	140	0.4	0.02
Meldin	15	200	1.0	0.035
SP-3	15	High Torque-Test Stopped		
SP-3	2.6	164	15	0.33
SP-211	15	High Torque-Test Stopped		
SP-211	2.6	140	1.5	0.09
SP-211*	2.6	102	1.0	0.05

* Runner chrome-plated

All other tests versus tungsten carbide

Conditions: dry N₂ atm. - 3600 rpm - 2450 fpm - 41 fps

Table 6-3 presents friction-wear data on these composites prior to and after exposure to NaK vapor and liquid. No significant, deleterious effect on these parameters was noted after such exposures. Based on the above experimental results, SP-211 was selected as the primary seal candidate material, with SP-3 considered its back-up. At this point in the program, therefore, fabrication of circumferential seal segments from these composites was initiated. Figures 6-6 through 6-9 are curves

TABLE 6-3
FRICTION-WEAR CHARACTERISTICS OF CANDIDATE SEAL MATERIALS
PRE- AND POST NaK EXPOSURE

Room Temp - 3 lb Face Load on 1/4" Face Line Contact

Material	Friction Coefficient			Wear Rate in mm		
	Before Exposure	After NaK Liquid	After NaK Vapor	Before Exposure	After NaK Liquid	After NaK Vapor
SP-211	0.27	0.17	0.30	2.7	2.6	2.6
SP-211	0.29	0.24	0.29	2.6	2.0	2.4
SP-3	0.35	0.35	0.35	3.7	3.9	3.9
SP-3	0.36	0.32	0.34	3.9	3.5	3.1

Note: Surface Velocity - 1250 fpm
NaK Exposure - 112-1/2 hours at 106°C

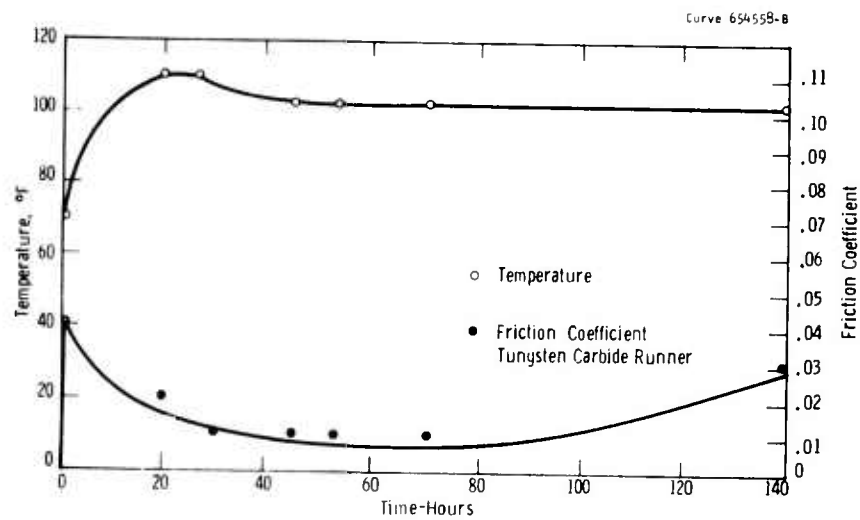


Fig. 6-6-Operating temperature and friction coefficient vs time for $WSe_2/GaIn$ seal material - 15 psi-2360 fpm- N_2

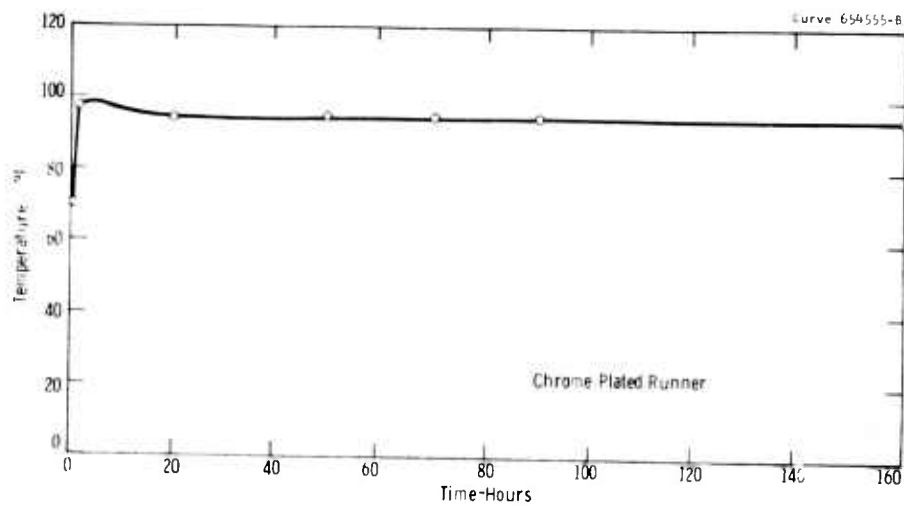


Fig. 6-7-Operating temperature vs time for SP-3 seal material - 2.6 psi-2360 fpm-He

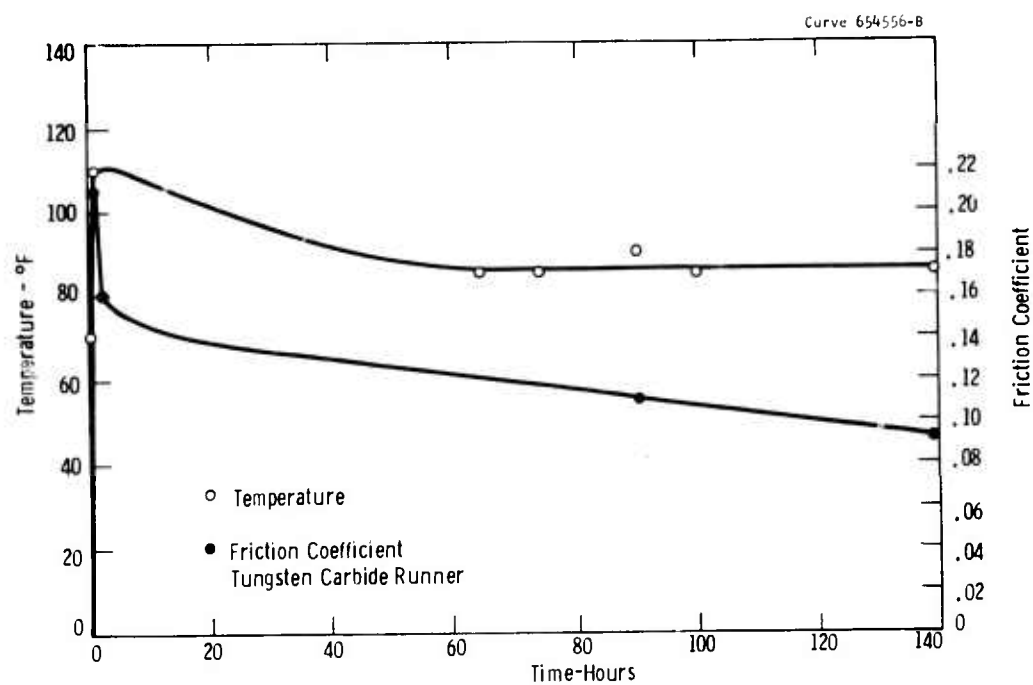


Fig. 6-8—Operating temperature and friction coefficient vs time for SP-211 seal material - 2.6 psi-2360 fpm- N_2

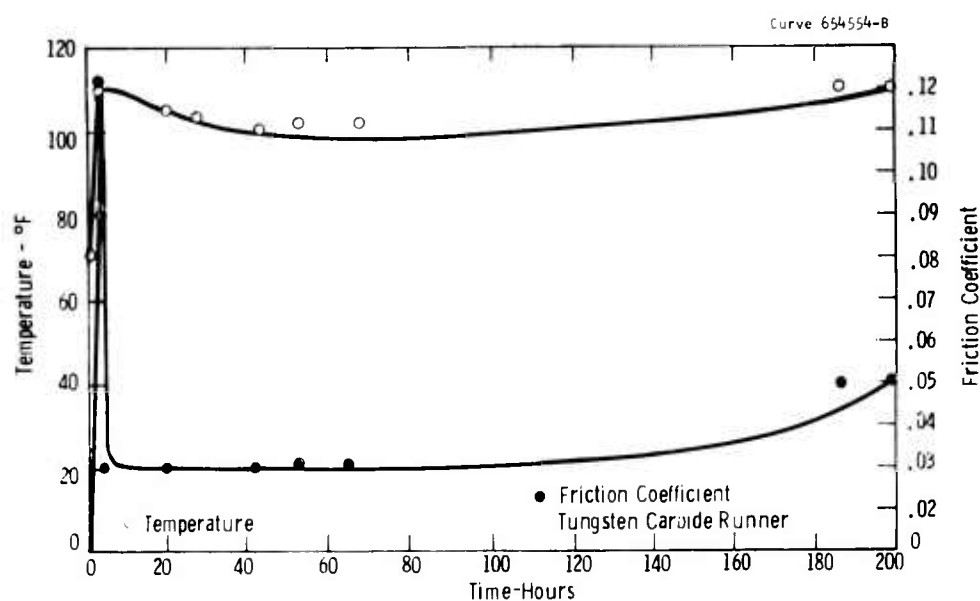


Fig. 6-9—Operating temperature and friction coefficient vs time for Meldin P1-30 seal material - 15 psi-2360 fpm- N_2

presenting friction-coefficient and operating temperature data versus running time for the various materials screened during this task.

6.2.2 Functional Testing: Tandem Circumferential Seal

Figure 6-10 is a photograph of a tandem circumferential seal designed and fabricated by the Metals Product Division, Koppers Company, Inc. Two of these units were purchased during this reporting period. In addition, two similar units of heavier construction were purchased from the Stein Seal Company, Philadelphia, Pennsylvania. Each unit consists of two circumferential seals made up of three segments each. Pertinent parameters of each seal are listed below:

	<u>Koppers</u>	<u>Stein</u>
Bore - inch	3.937	3.437
Outside Dia. - inch	5.697	5.697
Runner Width - inch	1.500	1.530
Gas Feed Pressure - psi	5	5
Seal Width	0.750	1.125
Shaft Dia. - inch	3.000	3.000
Runner Surface	Chrome plate	Tungsten carbide

In order to obtain bench mark performance data on standard seal designs, the first seals purchased were equipped with standard seal grades of carbon-graphite; namely, USG Grade 84 and USG Grade 67 for the Koppers and the Stein seals, respectively. The results of the first functional test performed on the Koppers seal design are presented in Figure 6-11 as a curve plotting seal leakage in cfm versus operating time. It will be noted that initially a leak rate of 0.095 cfm was observed with the seal operating at 2100 rpm and a 5 psig feed pressure of dry nitrogen gas. After approximately 2 hours of operation, this leak rate had decreased sharply to 0.025 cfm due to seal run-in and runner filming, and remained at this level for approximately 28 hours. At this point, however, abrupt and rapid wear of the seal material occurred, indicating carbon-graphite dusting, due to lack of moisture in its operating environment, and seal failure. The test result graphically illustrates the need to use seal materials that retain their self-lubricating ability in a no-moisture environment.

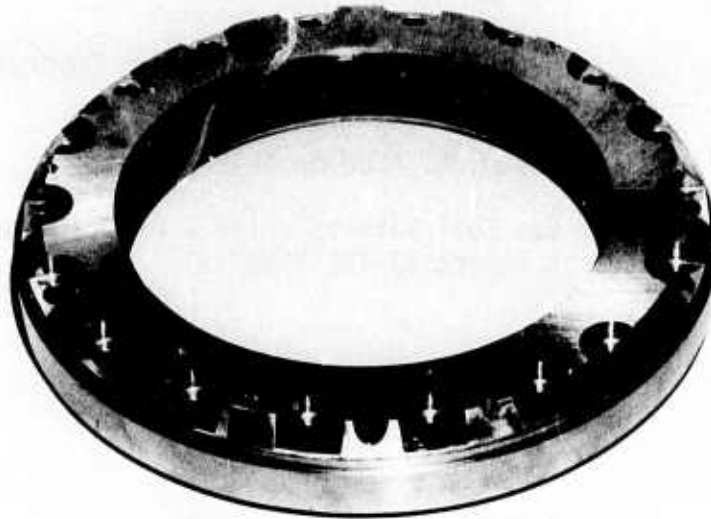


Fig. 6-10—Photograph of tandem circumferential seal-bore:
3.97" diameter

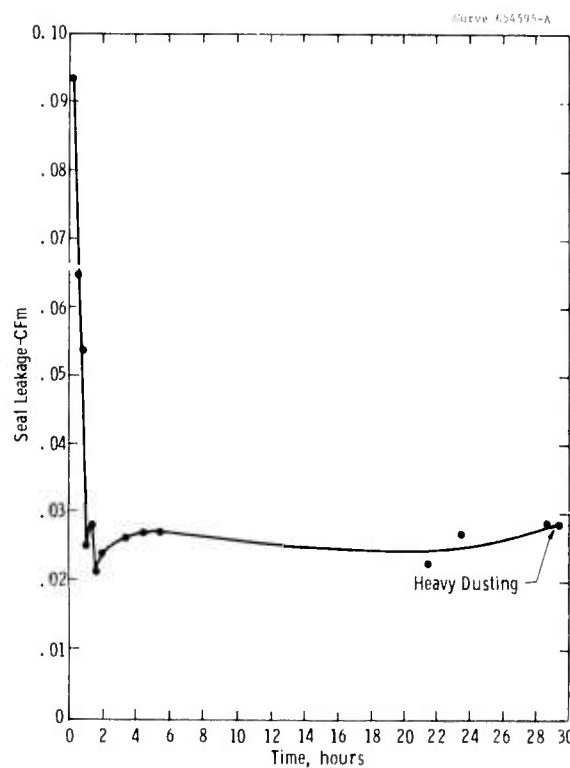


Fig. 6-11—Leak rate vs running time for Tandem Circumferential Seal
operating in dry N₂ 2100 rpm - 5 psig feed gas

6.3 REFERENCES

1. "Dynamic Sealing: Theory and Practice," Koppers Company, Inc., Baltimore, Maryland.
2. "Mechanical Seals," Mayer, E., London L1FFE Books LTD, 1969.
3. Bowen, P.H., "Cover Gas Seal Materials for a Liquid Metal Pump," Westinghouse Research Report 73-1B6-PUMAT-R1.